On the potting failure of inserts for sandwich panels: Review of defects and experimental analysis

Juan de Dios Rodríguez-Ramírez, Bruno Castanié, Christophe Bouvet

On the potting failure of inserts for sandwich panels: defects review and experimental analysis.

Juan de Dios RODRÍGUEZ-RAMÍREZ[1,*], Bruno CASTANIÉ[1], Christophe BOUVET[1]

[1] Institut Clément Ader (ICA), Université de Toulouse, CNRS UMR 5312-INSA-ISAE-SUPAERO-Mines Albi-UPS, Toulouse, France.

Abstract

In this paper the potting failures of inserts in sandwich structure is analyzed. The case of inserts potted with syntactic foam is investigated. First, a discussion about the influence of defects is made. Then, an experimental campaign is performed to determine the traction and compression behavior of the syntactic foam. Later, a specific technological pull-out test was performed, while a DIC system was used to record the tests. This allowed to observe and understand the different potting failure modes of inserts for sandwich panels. The obtained results suggest that the potting failure of inserts is predominant when fabrication or installation defects are present.

Corresponding author: jddrodri@insa-toulouse.fr

Keywords:

Inserts

Effect of defects

Sandwich structures

Potting

Syntactic polymer foam

1. Introduction

A sandwich structure consists of three main elements: two thin, stiff, and strong skins and a light thus mechanically weak core. Often, it offers a significantly higher bending and buckling stiffness compared to heavier laminates sheets. For this reason, it is used for aeronautical applications and the most used type of sandwich panel is with CFRP skins and Nomex® honeycomb core.

Nevertheless, until now these sandwich panels are restricted to helicopter fuselage, several business jets and secondary structures of commercial aircraft like cabin interiors or landing gear doors [1]–[7]. The main reasons are the complex design and the difficulty to ensure the quality requirements. Concerning their assembly, most of the time it is made through inserts with potting inside the honeycomb core (see Fig. 1) because the installation remains simple. However, an important problem of inserts is the complexity of the failure scenario when they are pulled out which is difficult to capture [4-7] without full 3D nonlinear finite element models. One of the issues is to decompose properly the failure scenario in the different parts of the insert (core, potting, skins …). According to the related literature [8], [9], the first component of the sandwich panel which is most likely to fail is the honeycomb core, which buckles due to the shear forces that it absorbs. However, this buckling can be elastic and reversible until some point, and it doesn't necessarily induce a global nonlinear behavior of the honeycomb structure. In addition, it's no easy to identify when the core starts to be permanently damaged as explained in [10]. Furthermore, the skins, the potting, and interfaces between each of the sandwich components might also be likely to fail depending on their dimensions and their respective stiffness and strength.

Moreover, besides the problem of the failure detection, the experimental evidence shows that the pull-out strength can vary significantly for inserts manufactured with the same specifications of size and materials. This aspect is very well known and has been already addressed by a few researchers. Smith et al, in [11], performed a reliability analysis that allows to better understand which are the parameters which can produce these strength variations. Their conclusions were that even if the first failure is caused by the buckling of the honeycomb core cells, the skins strength plays a very significant role. Also, Ragu et al, in [12], concluded that this variation was caused by the discrete nature of the honeycomb cells which causes variations in the potting shape and the thicknesses of the cell walls. In addition,

Slimane et al, in [13], performed an analysis of the pull-out strength variation versus the different possible potting shapes. To make things worse, the analytical approaches, proposed in the related literature of the ESA [14] or the US government [9] to estimate the pull-out strength, presents a significant lack of accuracy. This is also well known, and was addressed by Wolf et al in [15], where they performed a large study about the accuracy of this analytical method and showed that in average there is a difference of about -20% between the experimental and calculated strengths. They also used this approach in [16], where they evaluated different coefficients proposed by several authors in order compensate the lack of accuracy of this analytical approach. Summing up, the point of exact failure of inserts can be hardly identified, also, the discrete nature of the honeycomb causes significant pull-out strength variations, making even harder to establish a failure limit. And finally, the analytical approaches to estimate the pull-out strength might be not reliable. All these factors combined might lead to insert oversizing, or even to avoid the use of sandwich panels for certain applications.

For this reason, some investigations about inserts for honeycomb sandwich panels have been made in the last years, concerning their modeling [17], [18], analysis and calculation of the failure loads [15], [16] and the honeycomb core shear failure [10], [19]. Despite that, there are many aspects that still need some clarification. As explained previously, not only the core can fail, but also the potting or the skins. However, while the core shear or the skin failures have been already addressed by the scientific community, the pull-out potting failure remains to be investigated. There is experimental evidence that shows that the potting can fail before the core. Heimbs and Pein, in [20], and Yong-Bin Park et al, in [21], performed several inserts pull-out tests. For both investigations, they used two different full epoxy base systems without a lightweight filler. After having performed several insert's pull-out tests they cut the tested specimens in half (see Fig. 1). For the case shown in Fig. 1-a

the metallic insert is totally detached from the panel, while the Nomex core is not teared but apparently only buckled. This detachment may have been caused by a defective bonding of the metallic insert or because of the humidity and high temperature.

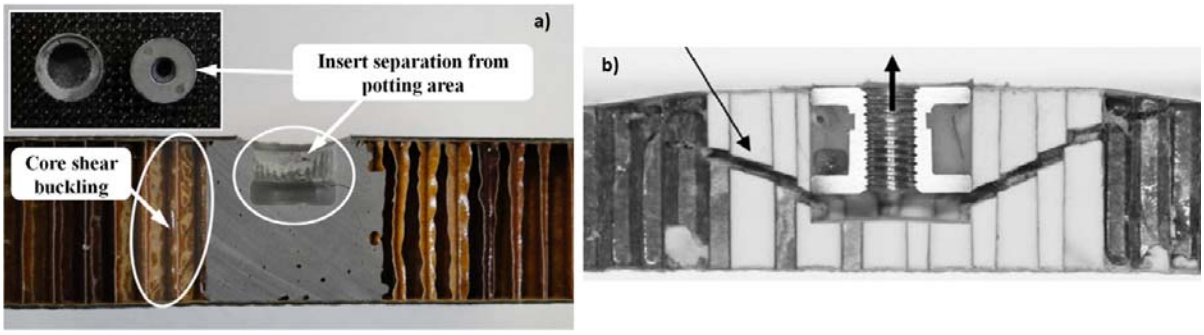

Fig. 1: Failure scenario after a pull-out test, reproduced from a) Yong [21], and b) Heimbs, [20].

For the case of Fig. 1-b the potting is broken and the core is ripped following the same path of the potting fracture, which suggests that the potting was broken first. A similar type of failure can be seen in the inserts tested by Bunyawanichakul in [22] where the potting compound was made of the Araldite AV121-N mixed with phenolic micro-spheres, a material that is often used in aeronautics and aerospace applications [23]. Once the pull-out test was performed, the postmortem specimens were cut in half to inspect the failure scenario (see Fig. 2). The specimens shown in Fig. 2-c) and d) presents a tensile failure of the potting, which propagates to the core. Since the potting stiffness is typically higher than the honeycomb core, the potting must have been broken before the core.

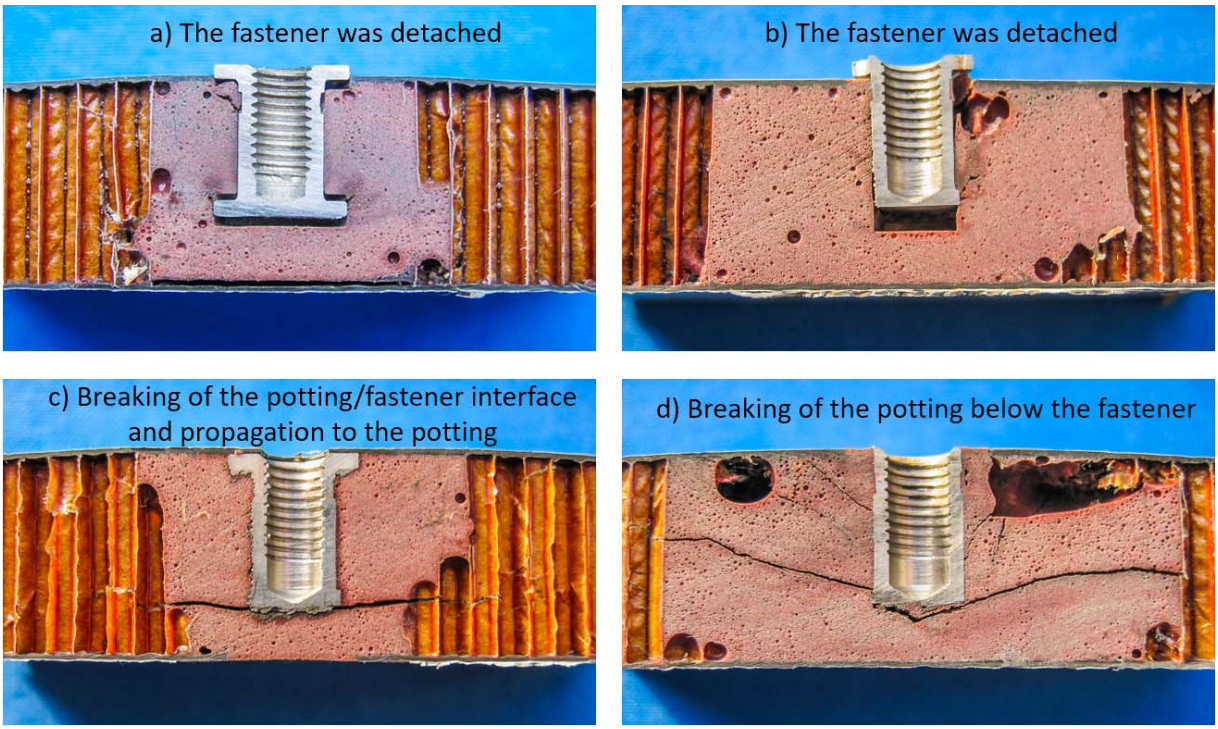

Fig. 2: Failure scenario after a pull-out test performed to different type of inserts [22].

For the other cases shown in Fig. 2-a) and b), the metallic insert was found to be detached from the potting, causing it to plasticize locally in compression. This might have been caused firstly by a breaking of the potting/metallic insert interface, that after been broken, allowed the metallic insert to be displaced, compressing the potting and obtaining the presented scenario.

All the presented evidences show that the potting can break before the core. For this reason, the insert design handbook of the ESA [14] proposes to estimate the insert pull-out strength based on the traction resistance of the potting. However, this approach might be too simplistic since it doesn't consider the influence of the different defects that might be present in the potting. Indeed, most of inserts are handmade and therefore they are very likely to be full of defects; like trapped air bubbles or unfilled sections. And this is particularly important because if these defects are combined with the variations originated by the discrete nature of the honeycomb cells, they might induce important variations on the potting size and thus the insert strength.

This research is a contribution to the understanding of the potting failure of inserts and is performed using a SPF (syntactic polymer foam) as potting but the conclusions could also be extended to full resin inserts. First, the most common defects that can be found in inserts are reviewed and a general discussion about their influence is presented. This allows to determine which ones are important enough to be considered for the insert design. Then, several technological pull-out potting tests specimens are manufactured while several intentional errors are made. This allows to establish a cause-and-effect relationship that helps to better understand the general procedure that leads to a defective potting, and in consequence, how to avoid it.

2. Discussion of potting defects influence in the pull-out strength

1.1 About the experimental evidence

Composite materials and structures are potentially subjected to many different type of defects, and it is shown in the literature that considering these imperfections for their design is very important (see for example [24]). Concerning inserts, only Raghu et al. in [12] have performed a study to evaluate the influence of defects, although only in a very small range. Beside this, there is not a quantitative analysis nor how these affect the insert strength, or how they should be considered for design purposes.

Nevertheless, performing a defect study of inserts could be very complicated, as it happens for most of composite parts, defects can't be completely seen and evaluated until the specimens are fabricated, tested and then cut to be analyzed. Also, there can be different type of inserts that can be installed into different types of sandwich configurations, and at least the most common configurations should be included into the study. In addition, since inserts are handmade, the introduced defects might vary according to the person and conditions under which the insert is installed, like pressure and room temperature.

This means that to perform a proper analysis, different persons should manufacture a huge number of different insert specimens, then tested them to obtain their strengths, and finally cut them to observe the defects. Without a doubt, this kind of study would require an important investment of effort, time and money.

To overcome this drawback, we thought that the evidence of other researchers can be used instead. This solves the problem because the specimens are manufactured by different persons, the inserts and sandwich types are different, but also the specimens are tested properly and the results are already reviewed and published. For this study, only publications presenting visual evidences are included and a summary of these are presented in Table 1. The number of collected evidences is 44.

	Skin				Core							Insert				Test	
	Reference	Thickness [mm]	E [MPa]	Poisson ratio	Reference	Height [mm]	G_W [MPa]	G_L [MPa]	t_adm W [MPa]	t_adm L [MPa]	Cell size [mm]	Potting reference	E [MPa]	Support radius [mm]	Potting radius [mm]	Failure load [N]	Failure criteria
Blind full potting (Kumsantia 2010)	G0939/145.8 [0/90]	0.55	52000	0.09	Nomex® honeycomb 3.0 pcf	20	17	26	0.32	0.48	3.18	EA9396 STRUCTIL - 10%mb phenol	940	30	16.5	1200	Aprox.
Through the thickness (Song 2008) P01	wsn3k SK chemical [45,0]s	0.84	49108	0.34	PN2-3.0-1/8	17.8	24	46	0.72	1.41	3.18	Hysol EA9394	4237	30	7.5	1890	First peak
Through the thickness (Song 2008) P02	wsn3k SK chemical [45,0]s	0.84	49108	0.34	PN2-3.0-1/8	22.9	24	46	0.72	1.41	3.18	Hysol EA9394	4237	30	7.5	2320	First peak
Through the thickness insert (Song 2008) P03	wsn3k SK chemical [45,0]s	0.84	49108	0.34	PN2-3.0-1/8	27.9	24	46	0.72	1.41	3.18	Hysol EA9394	4237	30	7.5	2640	First peak
Through the thickness (Song 2008) P04	wsn3k SK chemical [45,0]s	0.84	49108	0.34	PN2-5.0-1/8	17.8	42	74	1.48	2.24	3.18	Hysol EA9394	4237	30	7.5	2740	First peak
Through the thickness (Song 2008) P05	wsn3k SK chemical [45,0]s	0.84	49108	0.34	PN2-8.0-1/8	17.8	73	115	2.03	2.9	3.18	Hysol EA9394	4237	30	7.5	4480	First peak
Through the thickness (Song 2008) P06	wsn3k SK chemical [45,0,45]s	1.26	39437	0.47	PN2-3.0-1/8	17.8	24	46	0.72	1.41	3.18	Hysol EA9394	4237	30	7.5	2620	First peak
Through the thickness (Song 2008) P07	wsn3k SK chemical [45,0]2s	1.68	49108	0.34	PN2-3.0-1/8	17.8	24	46	0.72	1.41	3.18	Hysol EA9394	4237	30	7.5	3170	First peak
Through the thickness (Song 2008) P08	wsn3k SK chemical [45,0]s	0.84	49108	0.34	PN2-3.0-1/8	17.8	24	46	0.72	1.41	3.18	Hysol EA9394	4237	30	7.5	1840	First peak
Through the thickness (Raghu 2009)	2 plies 7781 E-glass/phenolic	0.51	2176	0.3	HRH-10-1/8-3.0	25.4	24.13	44.81	0.69	1.2	3.18	3M EC-2216 B/A Epoxy	-	40	10	-	-
Blind full potting (Raghu 2009)	2 plies 7781 E-glass/phenolic	0.51	2176	0.3	HRH-10-1/8-3.0	25.4	24.13	44.81	0.69	1.2	3.18	3M EC-2216 B/A Epoxy	-	40	10	-	-

Blind partial potting (Raghu 2009)	2 plies 7781 E-glass/phenolic	0.51	2176	0.3	HRH-10-1/8-3.0	25.4	24.13	44.81	0.69	1.2	3.18	3M EC-2216 B/A Epoxy	-	40	10	-	-
Blind full potting (Bin Park 2014)	Cytec 5250-4/T650-35 3K70PW [45,0,45]	0.65	47094	0.4	Gilcore HD322 2.0 pcf	25.4	11.7	20	0.31	0.552	4.76	Magnobond 6398	2068	40	10	1980	Core buckling
Blind full potting type 1 (Bunyawanichakul 2005)	G0939/145.8 [0/90]	0.55	52000	0.09	Nomex® phenolic 3.0 pcf	20	17	26	0.32	0.55	3.18	AV-121B-10%mb phenol	1312	30	9	1400	Aprox.
Blind full potting type 2 (Bunyawanichakul 2005)	G0939/145.8 [0/90]	0.55	52000	0.09	Nomex® phenolic 3.0 pcf	20	17	26	0.32	0.55	3.18	AV-121B-10%mb phenol	1312	30	18	1500	Aprox.
Full potting type 3 (Bunyawanichakul 2005)	G0939/145.8 [0/90]	0.55	52000	0.09	Nomex® phenolic 3.0 pcf	20	17	26	0.32	0.55	3.18	AV-121B-10%mb phenol	1312	30	9	2260	Aprox.
Through the thickness (Trap door Airplane) (Bunyawanichakul 2005)	G803/914 [0,45,]8s	2.6	41810	0.29	Nomex® honeycomb 3.0 pcf	20	24.13	31.71	0.55	0.8549	4.76	3M 3500-2B/A	1474	30	7.5	5500	Aprox.
Blind full potting (Heimbs 2009)	E-glass/ phenolic Stesalit PHG 600-68-50	0.24	20000	0.06	Schütz Cormaster C1-3.2-48	14.6	25.5	41.9	1.21	0.8	3.18	Cytec BR 632 B4/Huntsman Araldite 2011	3200	50	19	1978	Aprox.
Blind full potting (Seeman 2016) case 1	PHG 600-44-50 / PHG600-68-50 glass	-	-	-	Nomex® honeycomb 3.0 pcf	10	-	-	-	-	3.18	Ureol 1356 a/b	800	40	16.5	650	Aprox.
Through the thickness (Bianchi 2010)	Alu 2014	0.5	75000	0.3	5056 Alu 2.3 5.18pcf	19	220.6	579	2.06	3.44	6.35	Redux 219/2-NA	1034	40	7	5600	Max load
Blind full potting (Bianchi 2010)	Alu 2014	0.5	75000	0.3	5056 Alu 2.3 5.18pcf	19	220.6	579	2.06	3.44	6.35	Stycast epoxy 1090	2500	40	7	6180	Max load
Through the thickness (Wolff 2018)	Sigratex Prepreg CE 8201-200-45S [0,0,45,0,0]	0.85	52747	0.2	Plascore PAMG-XR1-4.5-1/8-10-P-5056	25	262	262	1.6	1.6	3.2	3M scotch Wld 2K DP490	-	30	13	7977	2% dev
Partial potting (Seemann 2018)	ABS5047-07	-	-	-	Nomex® phenolic 3.0 pcf	26	-	-	-	-	3.2	Epoxy base	-	40	-	1300	First peak
Through-thickness (Byoung 2008)	USN150, SK $[0/90]_{25}$	0.5	51700	0.28	5052 Alu 2.3 pcf	20	-	-	-	-	6.35	Stycast 1090	1200	35	7	3863	First peak

Table 1: Summary of insert pull-out tests considered for this study, information in empty fields is not available [5], [12], [27], [28], [16]–[18], [20]–[22], [25], [26].

By observing the different defects, it was clear that each type influences the integrity of the insert in a different way, for this reason, their criticality should be discussed individually. The first step is to classify them. Although there can be many ways to do this, the authors preferred to separate them into to the following four categories:

- Variations of the potting shape (see Fig. 3).
- A weak bonding of the metallic insert (see Fig. 7).
- Incomplete filling or presence of air bubbles in the potting (see Fig. 4).
- Irregular borders of the potting (see Fig. 6).

Then, to measure how these defects could affect the insert pull-out strength, several aspects could be evaluated, but for this study only four aspects are considered, they are:

- Frequency of appearance: If a defect is not very common, it could be ignored. In the other hand, if the defect is always present, its effect should be included for the insert design.
- Avoidability: The origin of defects is important. Defects that could be easily avoided should not be considered for the insert design.
- Influence on the insert strength: Some defects have more influence than others.

1.1.1 Variations of the potting shape

This irregularity appeared in 93% of the cases, due to the discrete nature of the honeycomb geometry as signaled by Raghu [12] or Slimane [13]. The potting shape is given by the cell size and the position of the perforation regarding the honeycomb cells. Since inserts are handmade, if the perforation is made slightly different, other cells are filled instead and the potting's shape may totally change. This means that the potting shape can't be controlled or predicted, therefore this defect can't be avoided.

This means that, even if the same tool is used to install two inserts in different places, the potting zone in both inserts might be different since it depends on the number of cell walls that are opened by the drilling tool (then filled with potting). And this is important because the insert pull-out strength depends on the size of the potting zone, as explained by most of the analytical models for the insert design [9], [14] .

To sum up, the fact that the size and shape of the honeycomb cells varies in the manufacturing process and that an insert is placed where is needed regardless of the honeycomb cell's positions makes their pull-out strengths different, even if the same materials and installation tools and are used.

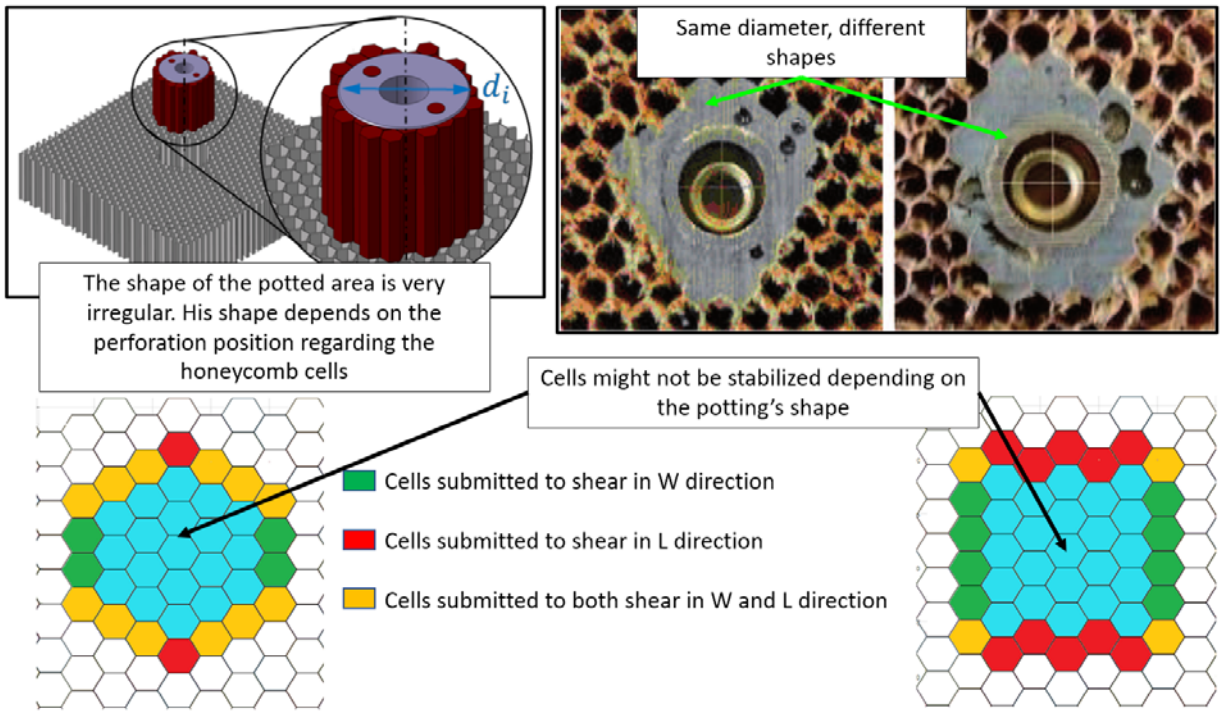

Fig. 3: Examples of variations of the potting shape for inserts, reproduced from [12], [16].

Moreover, the potting shape changes the distribution of the transversal forces, in consequence, it makes that the neighboring cells could be subjected to transversal shear in the W or L direction, or in both directions simultaneously depending of the insert geometry (see Fig. 3). This is important because the L direction shear strength is typically higher, and if there are more L oriented cells surrounding the potting, the strength could be increased. In the other hand, if there are more W oriented cells, the strength should be importantly decreased.

1.1.2 Incomplete filling and presence of air bubbles

This defect is very common as it appeared in 68% of cases. According to the ESA [14], it is caused when the potting viscosity is too high, or even because the injection was made too quickly. Thus, it can be due to a bad design or installation and can be avoided.

Air bubbles could have an important effect if they are placed next to the metallic insert, because they reduce the contact area, although they appear mostly far from it. However, most of the time, they don't affect the insert strength, even for big air bubbles. This can be seen in the test results of Bunyawanichakul in [22], where the insert strength for the

specimens named “type 2” presented a classical scatter of 20% of the insert strength, even if one specimen had a considerably big air bubble (see Fig. 4).

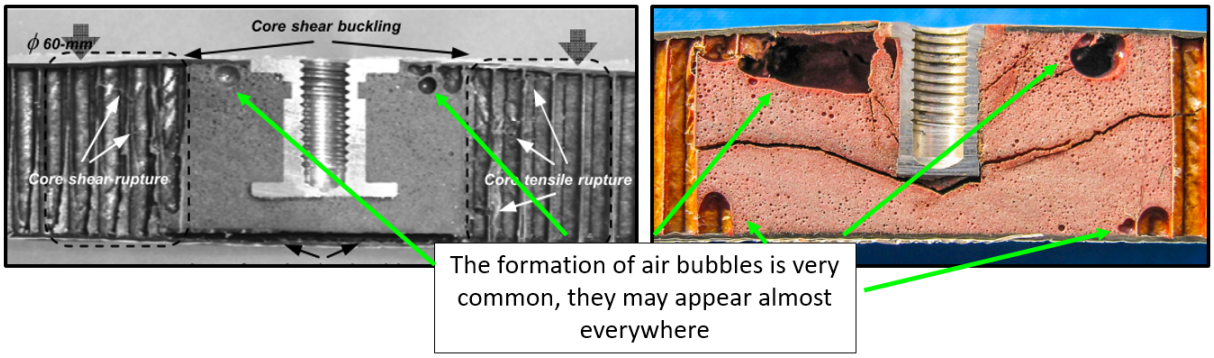

Fig. 4: Examples of the formation of air bubbles in inserts, reproduced form [22], [25].

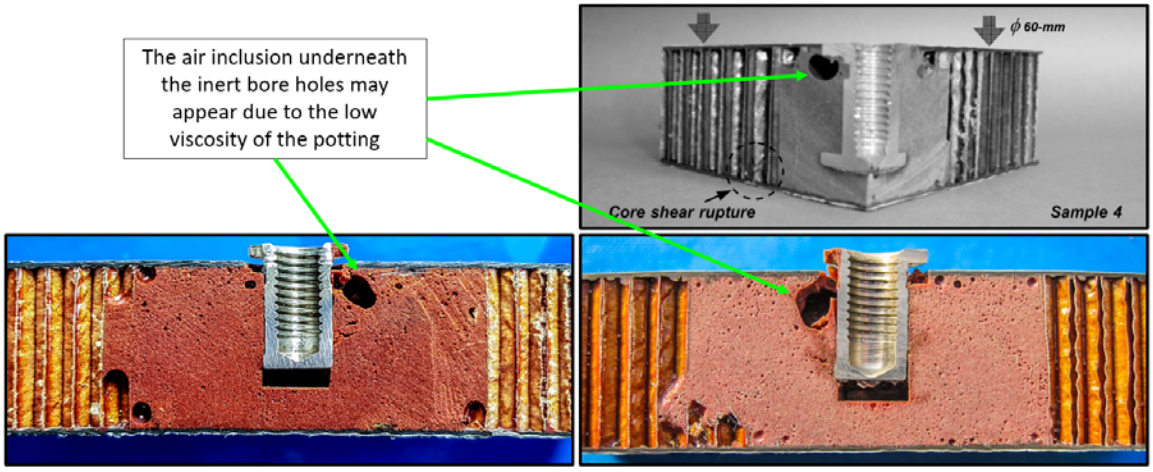

Fig. 5: Examples of incomplete filling underneath the metallic insert boreholes, reproduced from [22], [25].

1.1.3 Irregular borders of the potting

This defect appeared in 55% of the considered cases (see Fig. 6). It is caused by the partial removal of the honeycomb walls when the panel is perforated or when the undercut is made during the hole preparation.

Therefore, it might depend on the position of the perforation regarding the honeycomb cells but also of the perpendicularity of the drilling tool regarding the panel, especially when an undercut is performed to increase the potting zone and thus the insert strength. However, for a manual installation it should be very difficult to maintain the drilling tool perfectly

perpendicular to the sandwich, without mentioning this is impossible for curved panels. Nevertheless, this can also be caused by a rapid and careless installation when the undercut is performed, so it is difficult to say if this is avoidable or not.

The influence of this defect on the insert strength is that if the borders are irregular, hotspots are introduced into the cells surrounding the insert, which can affect the cells stability and reduce their strength.

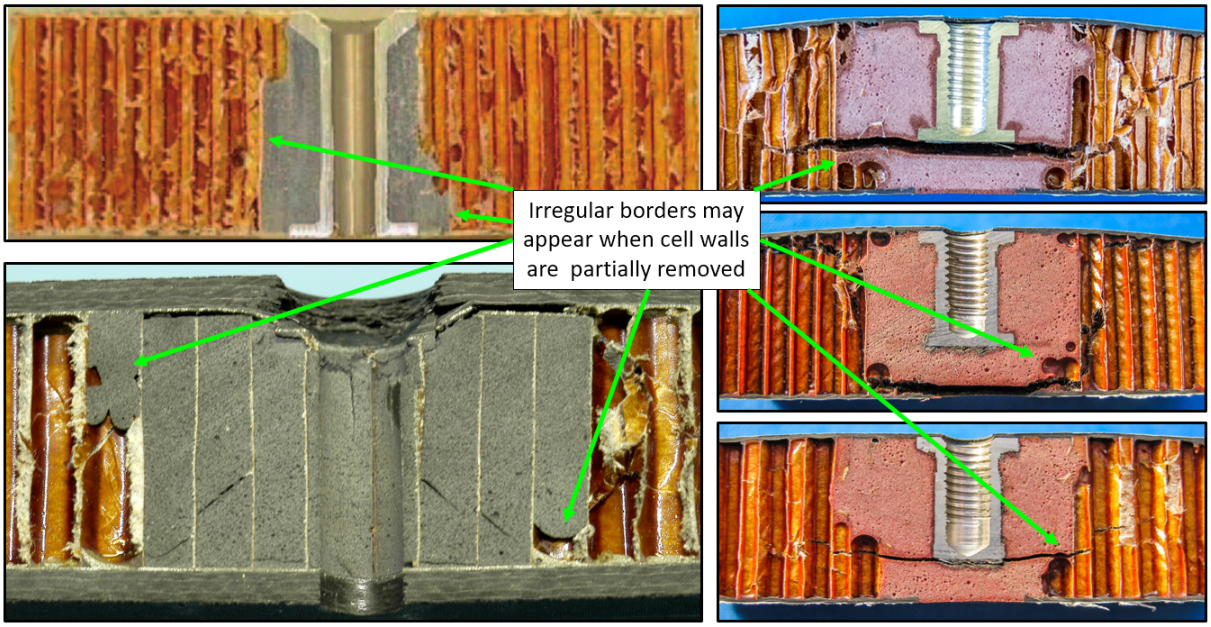

Fig. 6: Examples of the irregular borders formed in inserts due to partial removal of the honeycomb cell walls, reproduced from [5], [12], [22].

1.1.4 Defective bonding of the metallic insert

It appeared only in the 20% of the cases, it can be seen in Fig. 7. In the specimens of Bunyawanichakul (see ref. [22]) where a SPF was used as potting, and in the work of Yong-Bin Park where inserts were tested under high temperatures beyond 260° C (see ref. [21]).

The physical causes of this defect are not very clear and a deeper investigation is needed. However, it has a big influence on the insert strength, most of all because if the metallic insert is not well bonded, the load is directly transmitted to the contact zone between the metallic insert and the potting, which is often relatively small, causing the potting to break

or plasticize at very low pull-out loads. This aspect is relevant is addressed properly in the section 3

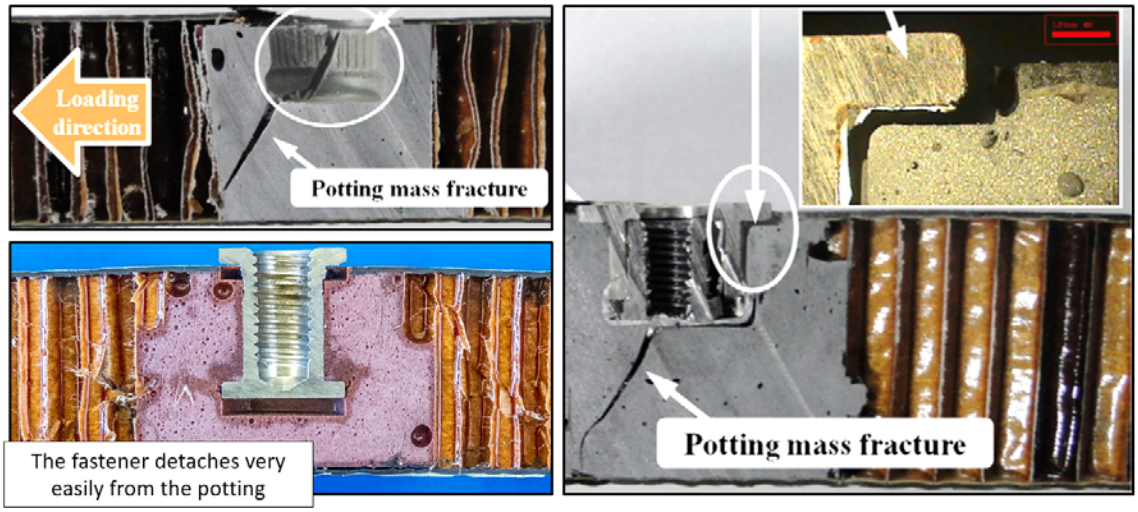

Fig. 7: Example of detaching of the metallic insert, reproduced from [21], [22].

1.2 Discussion about the criticality of defects

This study is useful to observe the frequency of the apparition of the defects. The most important one was the variation of the potting shape with an apparition frequency of 93%. Secondly, the presence of trapped air or incomplete filling of the potting appeared in 68 % of cases, followed by the irregular borders of the potting in 55% of the evidence, and finally the defective bonding in 20% of cases. Concerning the avoidability, the variations of the potting shape cannot be avoided. In contrast, the incomplete filling of the cells could be easily avoided if the viscosity of the potting is chosen properly and if the insert is carefully installed. Also, without a proper study no conclusions can be made concerning the defective bonding defect and the irregular borders of the potting. All these information along with the effects are summarized in Table 2.

At the light of this analysis, the variation of the potting shape should be considered for the insert design. The reason is because it appears almost for every case, it can't be avoided and it should have an important effect in the insert pull-out strength. Nevertheless, predicting

the potting shape may be very complex. A good way to do it is by estimating the range of the experimental scatter of the pull-out strength by considering the smallest and biggest possible potting surface for a given perforation hole.

Defect	Frequency	Cause	Avoidability	Effect	Should be considered for the design?
Variations on the potting shape	93.18%	Honeycomb shape	NO	Increases-Decreases the insert strength	YES
Incomplete filling or air bubbles in the potting	68.18%	Bad installation/ selection of the potting	YES	Apparently harmless	NO
Irregular borders of the potting	54.55%	Cell removal, undercut	NO	Should makesthe surrounding cells to collapse earlier	A proper study is required
Weak bonding of the metallic insert	20.45%	High temperature/microsphere oversaturation, studied in this research	YES	Damages the potting at very low loads	A proper study is required

Table 2: Analysis of the criticality of defects in inserts for sandwich structures.

As for the air bubbles or incomplete filling of the potting, its effect is mostly imperceptible and can be easily avoided. Thus, it might be irrelevant for the insert design.

Concerning the irregular borders of the potting, it is hard to tell about its avoidability and a deeper study is needed but is not performed in this research. And finally, about the weak bonding of the metallic insert, its effect is important and the causes might be too complex. Therefore, a deeper study is needed and is presented in the next section.

3. Experimental study of the defective bonding of metallic inserts

The insert detachment was found in two cases, the first one is when the pull-out tests were performed under high humidity and temperature and this was investigated by Yong-Bin Park in [21] and is not discussed in this paper. The second was in the tests performed by Bunyawanichakul in [22] when a SPF was used as potting, and this case is addressed here.

SPF are commonly used to imbibe metallic inserts into panels, allowing for bolted junctions. This foam accomplishes some main service functions like stress dissipation, protection of the core and the core/skin interface of the environment, and bonding of the metallic insert to the sandwich panel.

The potting is the key component of the insert technology, as it provides most of the desired protection functions. Concerning the material itself, it must be selected to be adhesively compatible with the other materials, be resistant to moisture and to isolate or protect the core from the exterior environment, to be strong enough to support the fatigue in the desired load range, but also to be lightweight.

SPF have been studied since the 60's and they were originally developed for deep submergence equipment or vehicles [29]. Therefore, they possess low density and high resistance to humidity, which makes them ideal as potting material for inserts. However, the mechanical behavior of these foams is difficult to predict because it is strongly influenced by several factors like the micro-spheres properties and its volume fraction, the fabrication procedure, etc. Also, their mechanical behavior is well known to be different in traction, compression or shear, due to the different failure modes of the microspheres that are activated: tensile fracture or debonding when the foam is submitted to traction [30], crushing of the microspheres when is submitted to compression [31]–[33], or a combination of them when is subjected to shear. Moreover, since the bonding mechanisms of adhesives are not yet very clear for the scientific community, the relation between the microsphere concentration and the adhesive capability of the foam remains to be investigated. Also, due to its nature, the microsphere distribution in SPF is random, so there can be spots where the concentration is higher and therefore the effective modulus of the foam is lower, or in the other hand, spots where the microsphere concentration is lower and the effective young modulus is higher. Moreover, when the metallic insert is pulled out, due to its shape, it submits the potting to complex stress until it fails. However, since the insert is hidden into the sandwich panel the way the failure appears cannot be seen and neither described or analyzed.

Summing up, to better understand the defective bonding of potting and metallic inserts, two major obstacles are detected. The first one is the complex behavior of the SPF

which varies depending of the microsphere concentration. The second one is due to location of the potting inside the sandwich and thus it is impossible to check experimentally the failure scenario. For theses reasons, the experimental approach is then divided in two test campaigns, the first one consists of traction and compression tests to determine the mechanical behavior of the SPF considering the microsphere concentration, while the second one consists of studying and observing the actual potting failure of the metallic inserts by performing several technological tests.

1.3 Study of the mechanical behavior of the SPF

The potting used in the work of Bunyawanichakul et al, in [22], is taken as reference. According to them, the SPF was made by mixing the Araldite AV-121 B epoxy adhesive with 15% of its ponderal weight with the HY 991 hardener and then adding 10 % of phenolic micro-spheres with an average diameter of 90 μm. The compressive modulus of this material was of 1312 MPa under compression and its density between 900 and 1000 kg/m^3. These properties were obtained after testing a cube of 10 mm by side under compression.

However, these mechanical properties might significantly change if the size of the testing specimen is reduced to a scale near the size of the microspheres, because of its random distribution. This is important because when inserts are being pulled out, the load is distributed mostly in the thin contact interface between the metallic insert and the potting, therefore only a very thin layer of foam is subjected to loading. Thus, the effective properties obtained through the testing of a massive block of potting performed by Bunyawanichakul might be not representative.

For this reason, since Bunyawanichakul claimed to have mixed the adhesive with phenolic micro-spheres at 10% of the ponderal weight, it was decided to study the behavior of the potting with 7, 10 and 13 % of its ponderal weight of micro-spheres which is equivalent to

a micro-spheres volume fraction of 42.2 %, 60.3 % and 78.5 %. This interval was considered reasonable to observe the effect on the mechanical properties of the microsphere concentration. The number of tested specimens was 18. This considers three different micro-spheres concentrations, tested in compression and tension and tested three times to obtain reliable results.

1.3.1 Fabrication of rod shaped specimens for compression testing

These specimens had the shape of a cylindrical rod and their height was the double of its diameter as recommended by the ASTM D695. All the specimens were fabricated using a syringe which was filled with potting carefully to avoid air bubbles. Then, the potting was left to polymerize at room temperature for 6 days. After that, the material was extracted from the syringe with compressed air and cut to the desired size in a lathe. Special care was taken in this last step to obtain uniform faces. Finally, the specimen's dimensions were 6.11 mm of radius by 24.9 mm of height (see Fig. 8).

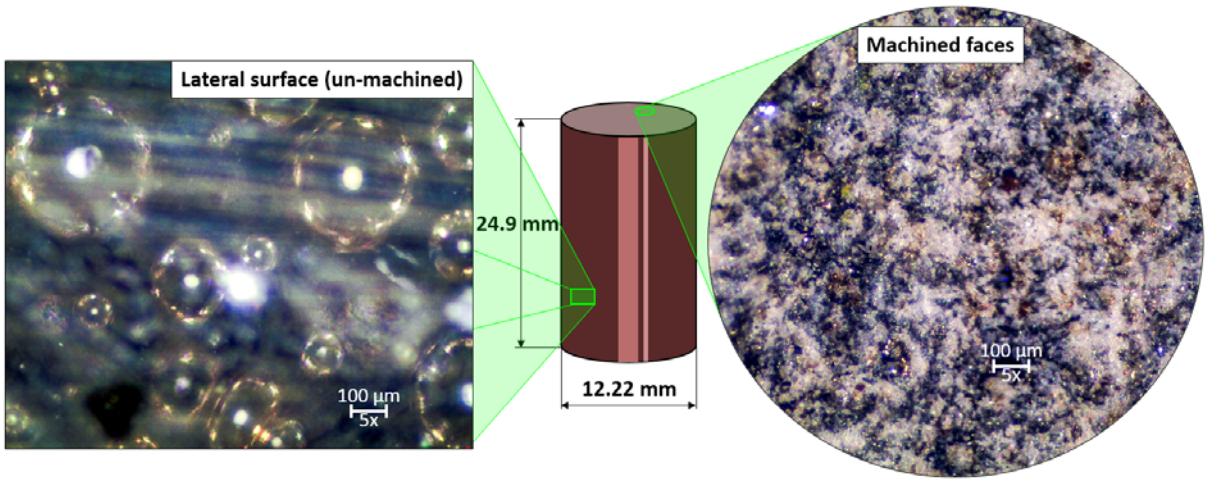

Fig. 8: Size of the compression specimens and view of the surfaces under the microscope.

Since the fabrication required dispersing all the micro-spheres in the adhesive, the paste was stirred intensively several times, although no special care was taken to leave intact the micro-spheres. Therefore, to verify that they were not damaged, the exterior surfaces of the specimen were inspected under the microscope.

In the plane surfaces, there was no trace of the micro-spheres, all were broken by the lathe, which is normal. For the cylindric surface, intact micro-spheres were seen inside the polymer (see Fig. 8).

1.3.2 Fabrication of "Dog Bone" shaped specimens for tensile testing

For the tensile tests, the recommendations of the ASTM D638 were followed. A specific shape for the traction specimens was used, commonly called dog bone. The dimensions of the specimen are shown in Fig. 9. This shape allows minimizing the effect of stress concentrations.

The specimens were fabricated using a mold made of wood. For all the specimens, the potting was left to polymerize for 6 days at room temperature. Initially, the thickness of the specimen was of 10 mm, but unfortunately due to the maximal opening of the testing machine clamps, this thickness had to be reduced through milling to 7 mm. Finally, the specimens were painted with speckles to be analyzed with a 3D digital image correlation system.

For the tensile tests four specimens of each type were fabricated although only 3 were tested. This was just in case one specimen breaks in the demolding process.

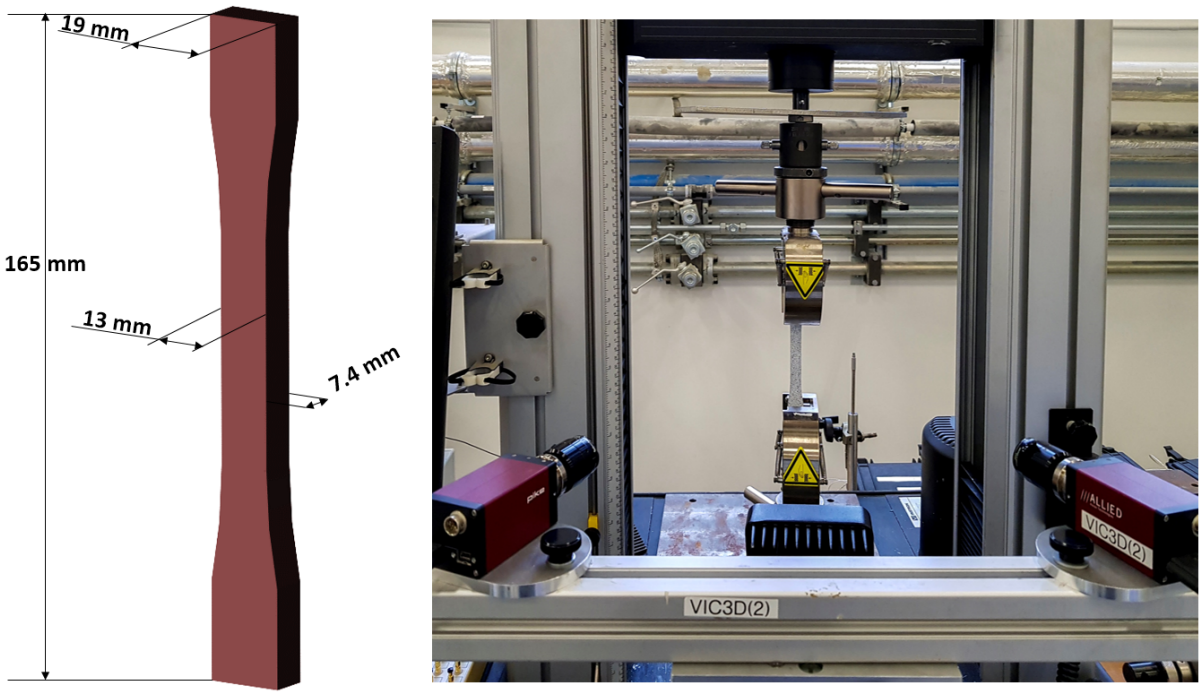

Fig. 9: Shape and set up of the traction test specimens.

1.3.3 Test setup

All the specimens were tested using an Instron 10 kN machine. For all the tests, the force was measured directly from the machine and the machine speed was set to 0.5 mm/min.

For the compression test, two rectified metal blocks were used between the machine and the specimen to ensure the contact and parallelism. An external LVDT sensor was used to measure the displacement of the machine. For the tensile specimens, a 3D DIC system was installed to measure the deformation field in the plane of the specimen. One image was taken every two seconds.

1.3.4 Test results and discussion

The test results are shown in Fig. 10 and Fig. 11 for tension and compression respectively. The specimens with different percentage of micro-spheres are speared by color; blue for 7%, yellow for 10 % and green for 13%.

In tension, the average elastic moduli were 2190, 1851 and 1670 MPa for 7, 10 and 13% of micro-spheres weight respectively. In the same order, the loss of linearity started at

10, 9.5 and 9 MPa and the tensile failure occurred at 17.4, 15 and 13.8 MPa (see Fig. 10 and Table 12).

Micro-spheres ponderal weight	0 %	7 %	10 %	13 %
Micro-spheres volume fraction	0 %	42.2 %	60.3 %	78.5 %
E_t [MPa]	4000	2190	1851	1670
Loss of linearity traction [MPa]	unknown	10	9.5	9
$\sigma_{t\,max}$ [MPa]	19	17.4	15	13.8

Table 3: Summary of the test results for the traction tests of the potting.

Micro-spheres ponderal weight	0%	7%	10%	13%
Micro-spheres volume fraction	0 %	42.2 %	60.3 %	78.5 %
E_c [MPa]	4000	1291	1233	1226
Loss of linearity compression [MPa]	unknown	20	19	17
$\sigma_{t\,max}$ [MPa]	unknown	34	31.5	30

Table 4: Summary of the tests results for the compression tests of the potting.

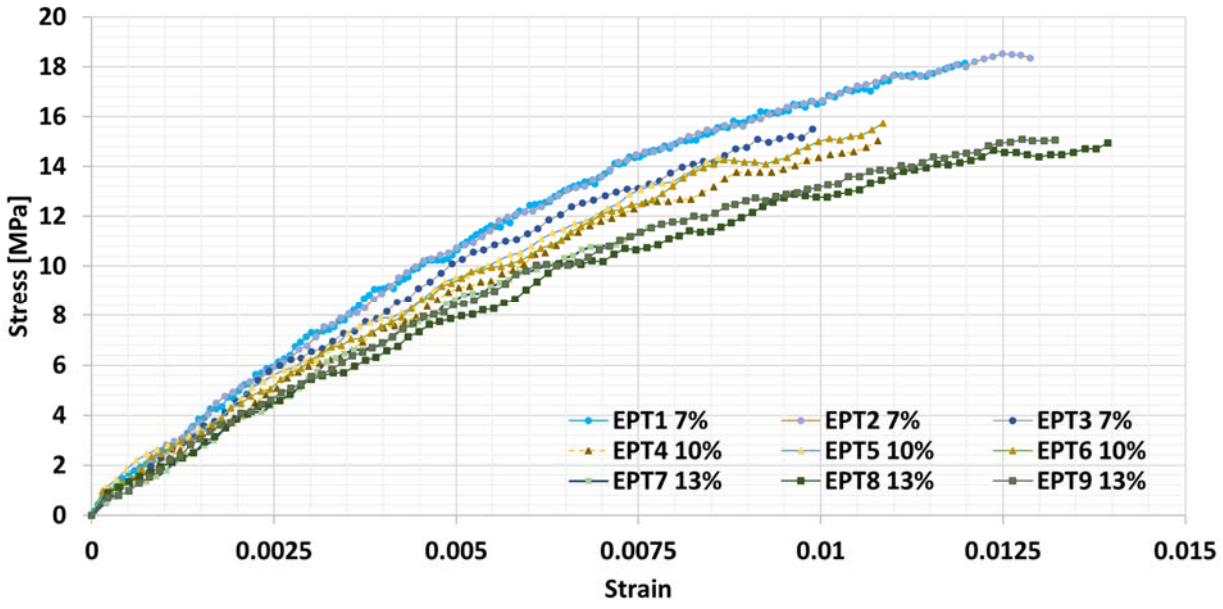

Fig. 10: Experimental curves of the tensile tests of the potting.

The averages in compression were 1291, 1233 and 1226 MPa for 7, 10 and 13% of the micro-spheres weight respectively, also, in the same order, the loss of linearity started at 20, 19 and 17 and the specimens presented a perfectly plastic behavior at 34, 31.5 and 30 MPa respectively (see Fig. 11 and Table 13).

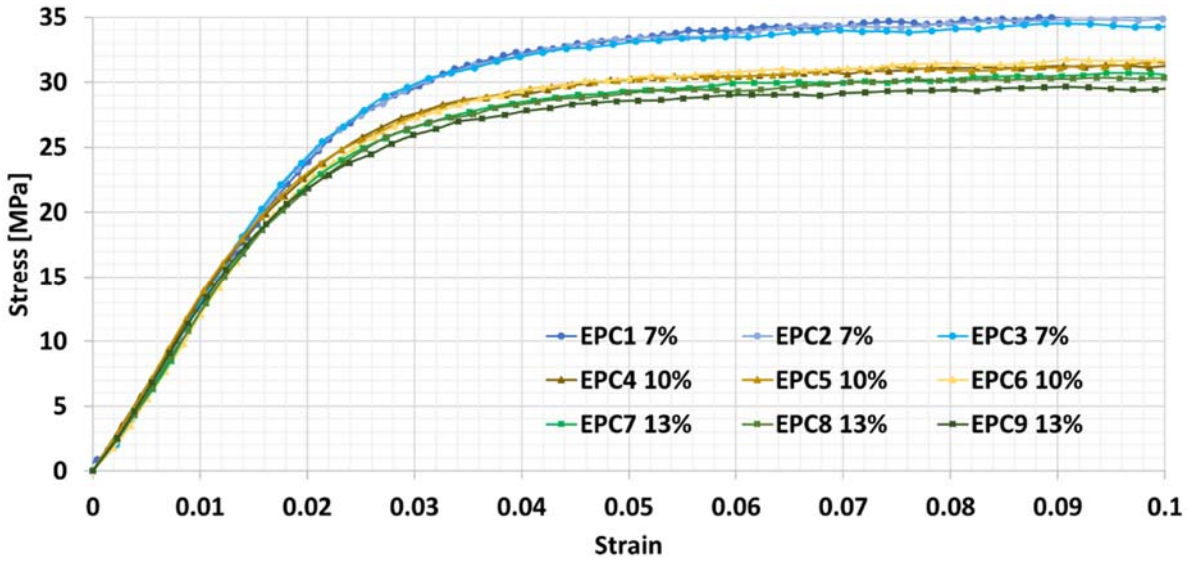

Fig. 11: Test results of the compression tests of the potting.

The first remark is that the elastic moduli in compression and tension were different which is characteristic of these foams. Also, the percentage of micro-spheres used in the potting fabrication clearly influenced the elastic modulus. The foam became stiffer when the micro-spheres volume fraction was smaller, and vice versa.

Concerning the compressive effective elastic modulus, it was almost independent of the microsphere concentration, but the maximum shear stress is reached when less microspheres were used for the foam. Also, it is worth mentioning that when the foam is crushed, it presents an almost perfectly plastic behavior.

In contrast, the traction elastic modulus and strength of the foam were significantly sensitive to the microsphere concentration. They increased while the microsphere concentration was reduced. Moreover, the material presented a brittle fracture instead of plasticity when it failed.

Finally, considering the supplier values of the adhesive, the compression tests made by Bunyawanichakul and the results of the tests performed in this study, the data about the mechanical behavior of the foam is shown in Fig. 12 and Fig. 13.

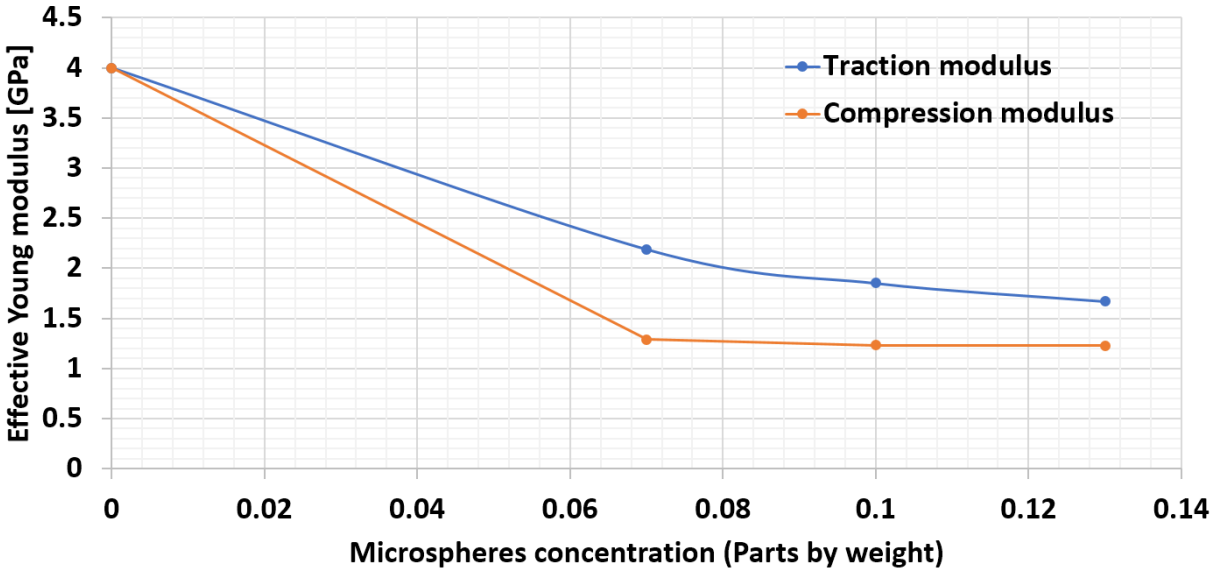

Fig. 12: Experimental effective Young moduli in traction and compression as function of the micro-spheres concentration.

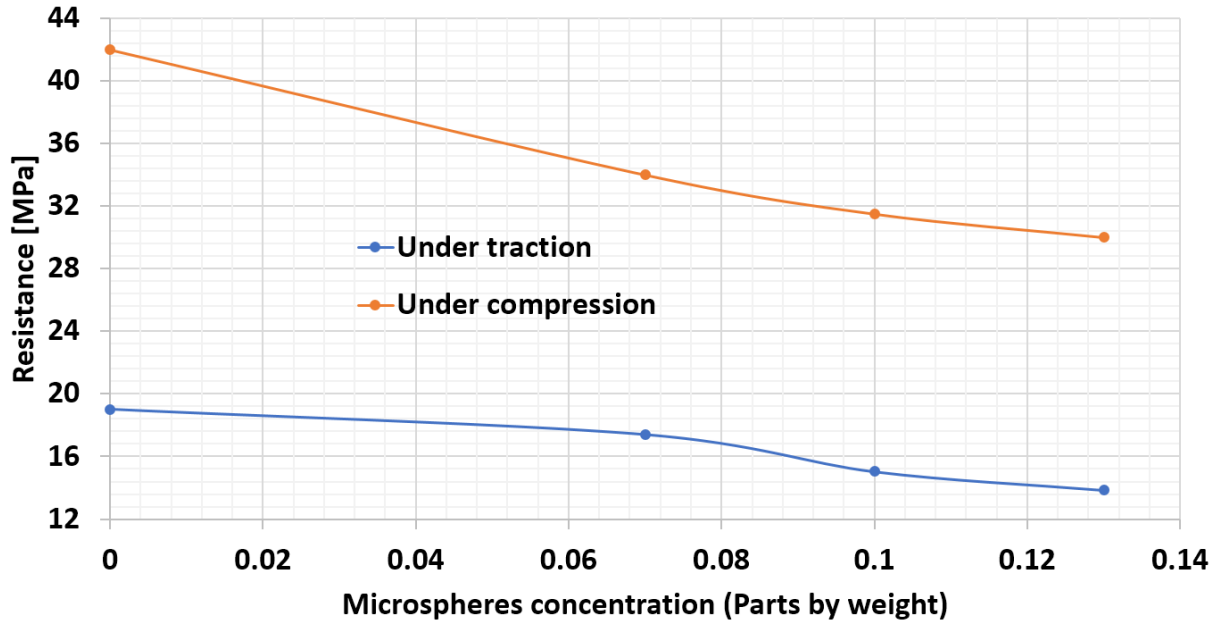

Fig. 13: Resistance to failure under traction and compression as function of the micro-spheres concentration.

1.4 Technological pull-out tests

The second part of the experimental study consisted into analyze the potting failure of the inserts tested by Bunyawanichakul in [22]. However, the main problem is that the actual failure can't be seen because it happened inside the sandwich panel.

To overcome this problem, it was considered that the insert failure scenario was very similar from any diametric cutting plane of the insert. Indeed, although the evidence shows some small differences (see Fig. 2, Fig. 4, Fig. 5 and Fig. 6), for practical terms the failure can be considered as symmetric. Then, this hypothesis makes possible to substitute the "cylindrical" shape (with diametric symmetry) by a rectangular shape (that possess orthogonal symmetry). This is advantageous because while for the cylindrical shape the insert remains hidden, in the rectangular shape the exterior borders can be exposed and thus, the failure can be observed. Then, to reproduce similar failure modes of those found by Bunyawanichakul, the next step was to conceive a technological test that submits the potting to similar loading as in the insert-pull out test. For this purpose, four types of specimens were used in this study and they are shown in Fig. 14.

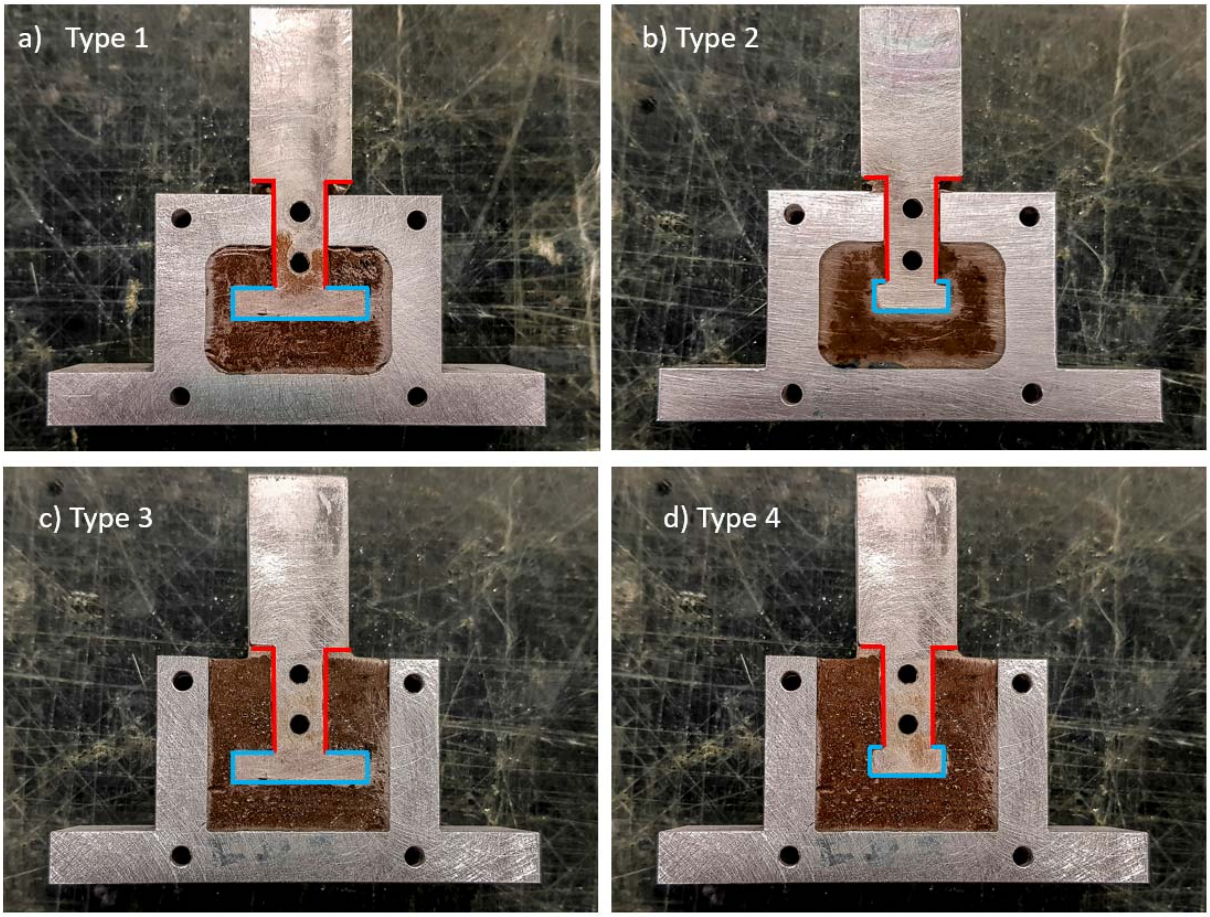

Fig. 14: Test specimens subjected to pull-out.

They consist of a metallic piece that represents the insert, and is surrounded by the potting material as it happens for insert. Each specimen privileges different aspects, and this is intentionally made to stablish a cause-effect relation between these aspects and the failure modes.

- On the specimen type 1 the metal rod/potting interface was very large, therefore we expected to see a failure of the potting, due to compression or traction and shear.
- On the specimen type 2 the surface of the interface metal rod/potting was smaller and we expected to see this interface break.
- On the specimen type 3 the conditions were like the type 1 test, but the potting container box was open, so the potting was subjected pronominally to traction.
- For the type 4 the interface metal rod/potting was subjected to traction and shear, but the box was open.

Also, since the influence of the micro-spheres concentration for the potting failure is unknown, it's included as a variable in this study. For this reason, different percentage of micro-spheres were used to fabricate the 16 specimens, going from 10% to 15%.

1.4.1 Specimen's fabrication

To obtain the four types of specimens, only two different metal rods and two different type of boxes were manufactured. Also, it is worth mentioning that they had 25 mm of thickness which was considered enough to reduce the influence of the free border effects (see Fig. 15).

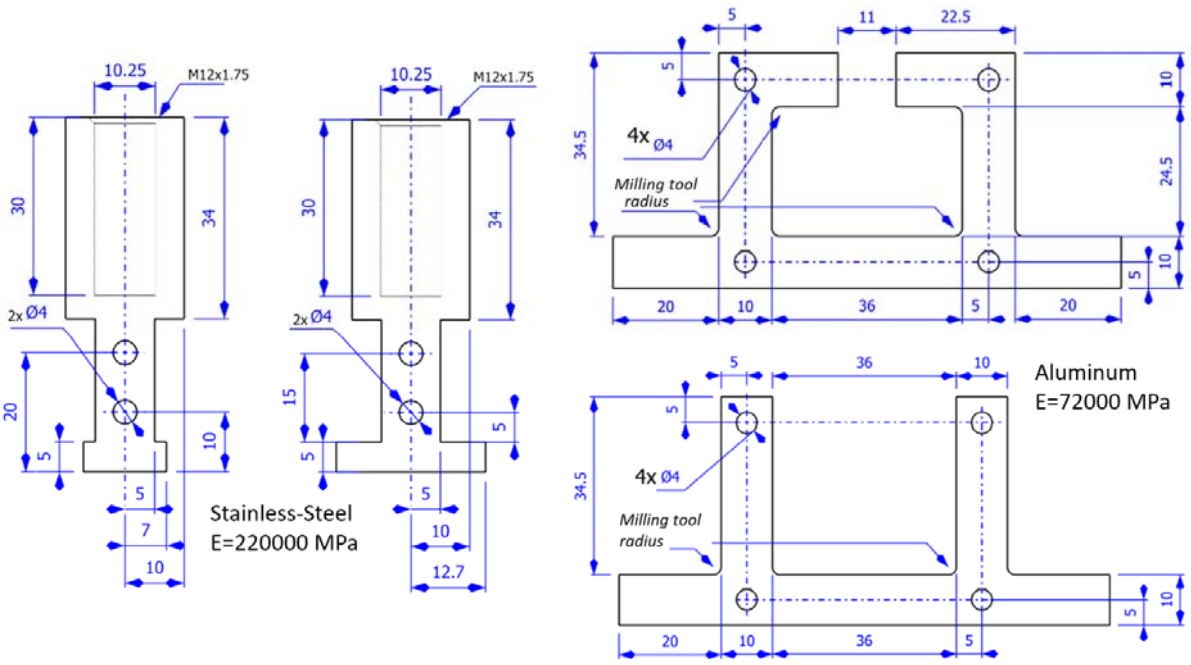

Fig. 15: Geometry of the rods and potting containers.

The metal rods were made of stainless steel to represent the insert. The boxes that contained the potting were made of aluminum and provided a similar fixation as when the potting is imbibed in the sandwich panel. Since the number of metallic parts was reduced, the tests were made gradually. First, a few specimens were tested to see if the results were as expected, then the potting fabrication was adapted at each time to try to obtain the desired failure scenarios. All this process, combined with the fact that the tests provided very different evidences, resulted in a very random number of specimens of different characteristics.

The potting was a SPF that consisted of the epoxy adhesive araldite AV-121-N mixed with the HY 991 hardener, and the microsphere concentration varied from 10 to 15% of the mixture ponderal weight. For some specimens, the stainless-steel rod was not degreased to see how this affected the results of the tests. Moreover, for some specimens an excess of hardener was mixed on purpose to observe the variation of the mechanical properties of the resulting compound, this variation is attributed to human error on the handmade manufacturing.

Then, the interfaces showed in red in Fig. 14 were covered with a Teflon tape to avoid the adhesion. This made easier to analyze the results of the tests because the deformation of

the potting was caused only by the end of the metal rod. Once the SPF was stirred and ready to be used, the metal pieces were assembled and then filled with potting.

Finally, specimens EP13 to EP16 were left to polymerize at 40° for 1 hour and specimens EP17 to EP20, were left to polymerize at room temperature, as for the remaining samples, they were polymerized at 100°C.

All the characteristics of each specimen are listed in Table 5. They are sorted by specimen type, from 1 to 4 (column two). The first four corresponds to the specimen description, name of the specimen, type, percentage of microspheres and observations. The associated colors are to identify the specimens that were made the same day. Columns five and six are explained in the test results and discussion section.

Specimen	Type	% of micro- spheres	Observations	Max load [KN]	Failure mode
EP3	1	11	Left at 100°C 1 hr.	7.658	A
EP4	1	13	Left at 100°C 1 hr.	7.732	A
EP6	1	15	Not degreased, left at 100°C 1 hr.	-	C
EP10	1	15	Left at 100°C 1 hr.	2.908	B
EP13	1	12	Left at 40°C 1 hr.	-	C
EP20	1	11	Left at room temp.	10.0	A
EP2	2	11	Left at 100°C 1 hr.	5.005	A
EP7	2	15	Not degreased, left at 100°C 1 hr.	-	C
EP12	2	15	Left at 100°C 1 hr.	-	C
EP16	2	12	Left at 40°C 1 hr.	-	C
EP17	2	11	Left at room temp.	6.25	A
EP1	3	10	left at 100°C 1 hr.	8.15	A
EP9	3	15	20% more of hardener, left at 100°C 1 hr.	6.108	B
EP14	3	12	Left at 40°C 1 hr.	8.9	A
EP19	3	11	Left at room temp.	8.675	A
EP5	4	13	Left at 100°C 1 hr.	5.765	B
EP8	4	15	Not degreased, left at 100°C 1 hr.	2.886	B
EP11	4	15	20% more of hardener, left at 100°C 1 hr.	2.956	B
EP15	4	12	Left at 40°C 1 hr.	3.6683	B
EP18	4	11	Left at room temp.	6.9	A

Table 5: Summary of the potting pull-out test campaign.

1.4.2 Technological test setup

Once the specimens were manufactured, they were painted in white with black speckles. A 100 kN Instron machine was used to test the specimens. The specimens were fixed using clamps as shown in Fig. 16. Then the displacement was imposed from the inferior

part of the machine while the superior part was fixed. A DIC 3D system was used to measure the displacement field of the test specimen. The images were taken with a frequency of 2 Hz. The force signal was measured directly from the machine while the applied displacement was measured by calculating the average of the vertical displacement in points P1, P2, P3 minus the displacement at P4 (see Fig. 16).

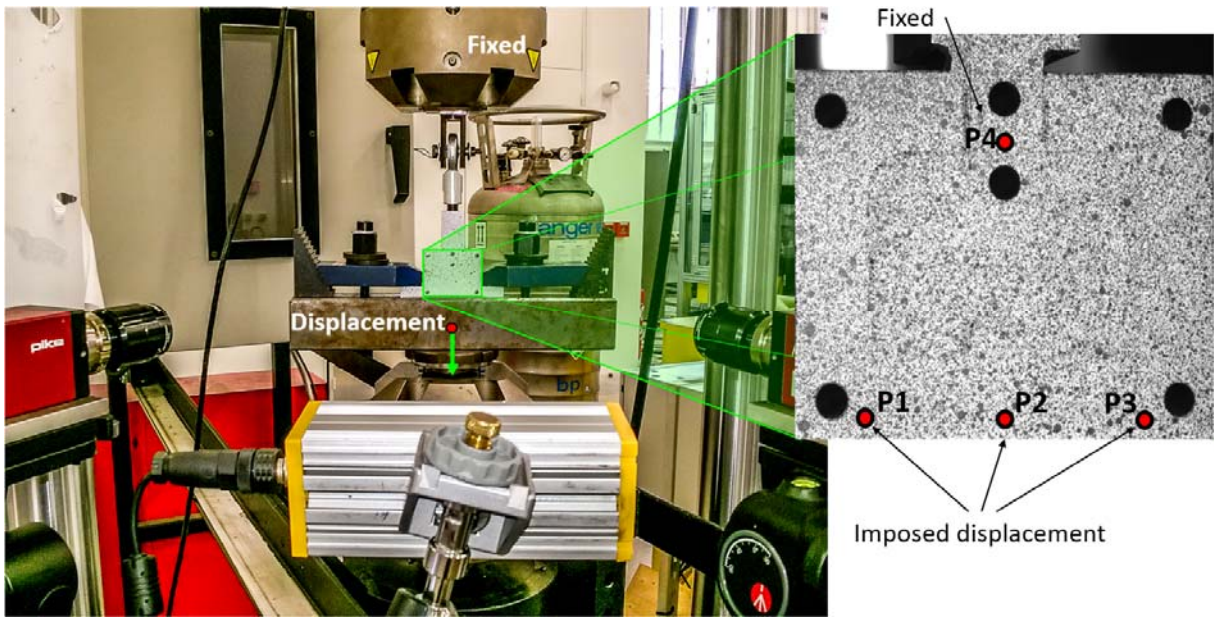

Fig. 16: Test set up and measuring of the pull-out displacement of the rod.

1.4.3 Tests results and discussion

Once the tests were made, the obtained data was analyzed and compared. The results are presented by specimen type. Concerning the specimens' type 1, EP3, EP4 and EP20, the activated failure mode was a sudden brittle breaking of the potting below the metal rod. On the EP10 specimen it was the breaking of the metal rod/potting interface and propagation of the fracture. For the specimens EP6 and EP13 the metal rod was not bonded to the potting and therefore the load was concentrated in the contact zone between the metallic part and the potting, which resulted into a gradual and slow crushing of the foam without sudden breaking (see Fig. 17).

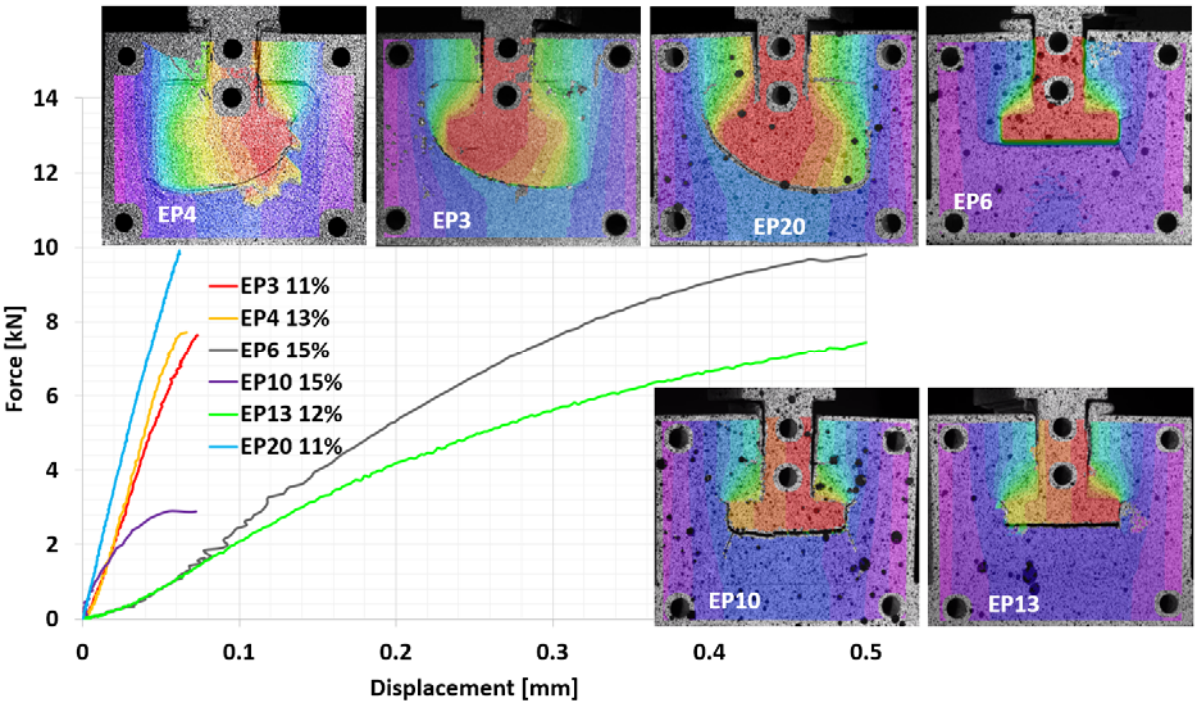

Fig. 17: Experimental results of the test specimens type 1.

As for the specimens' type 2, EP2 and EP17 specimens presented a failure of the potting below the metal rod. For the specimens EP7, EP12 and EP16 the steel rod was not bonded to the potting and the foam was slowly crushed without an abrupt failure (see Fig. 18).

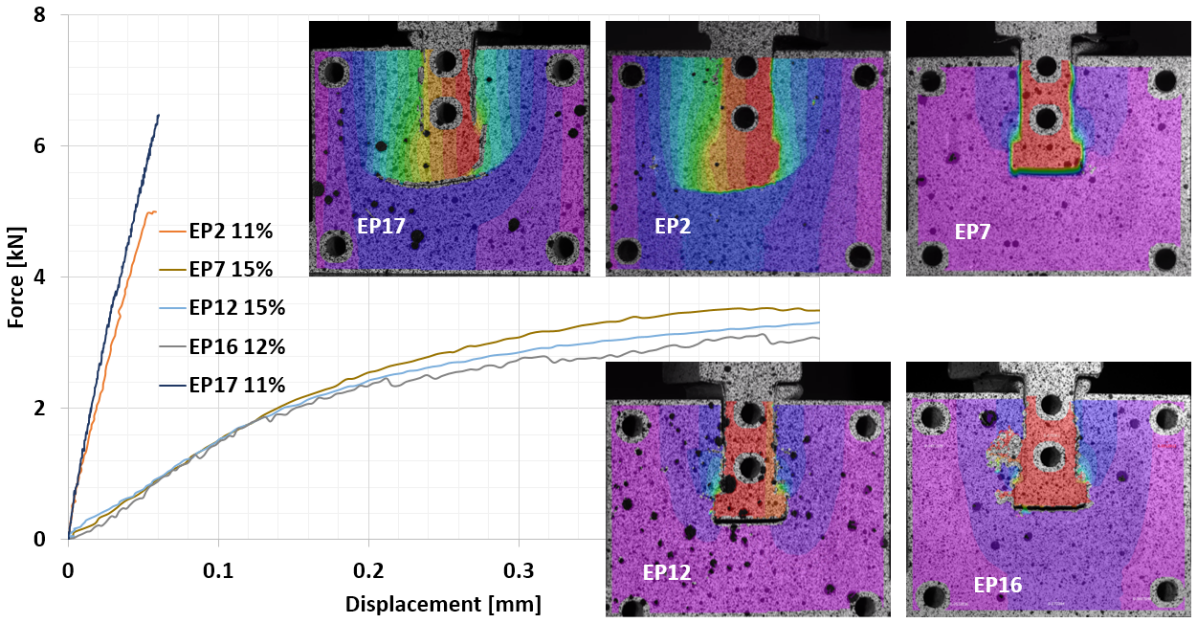

Fig. 18: Experimental results of the test specimens type 2.

For the specimens' type 3, EP1, EP14 and EP19 the failure was caused by the breaking of the potting below the metal rod. For the specimen EP9 the failure was the breaking of the interface between the steel and the potting (see Fig. 19).

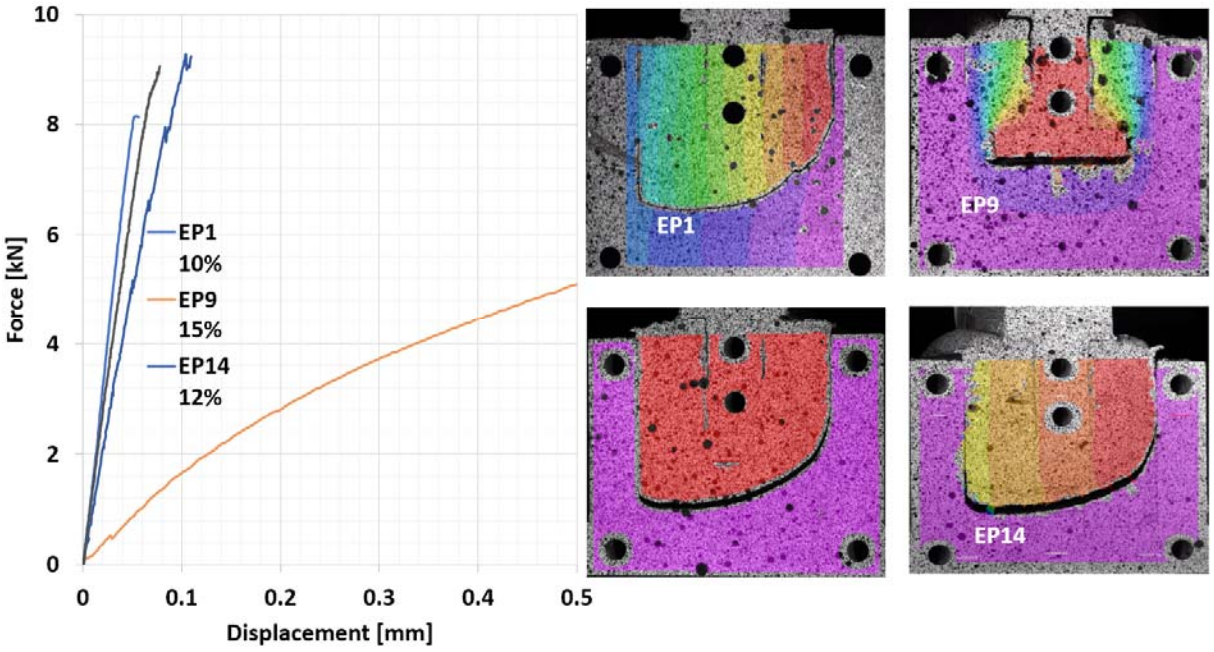

Fig. 19: Experimental results of the test specimens type 3.

Finally, for specimens' type 4, the specimens EP5 and EP18 presented the breaking of the metal rod/potting interface with propagation of the fracture into the potting. The failure of specimens EP8 and EP15 was a combination of the breaking of the potting and the breaking of the interface between the rod and the potting; finally, EP11 failed due to the breaking of the potting rod interface (see Fig. 20). It is not possible to isolate and obtain each failure mode because several failure mechanisms are activated simultaneously. Nevertheless, the authors thought that it was possible to separate them into three types:

- A: Brittle breaking of the potting below the rod (color blue of the failure mode column)
- B: Breaking of the interface potting/rod (color green of the failure mode column)
- C: Not bonded (color yellow of the failure mode column)

All specimen characteristics and failure modes are summarized in Table 5.

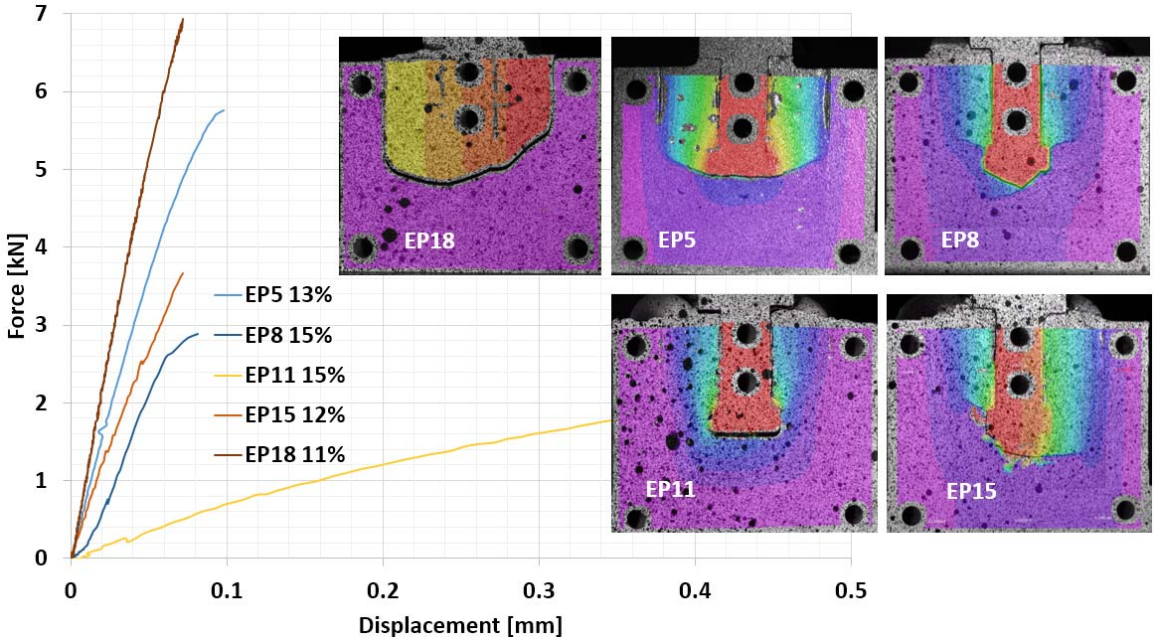

Fig. 20: Experimental results of the test specimens type 4.

Visibly, all the failure modes observed in the insert tests of Bunyawanichakul were also present in our tests. Nine specimens (EP1 to EP4, EP14, EP17 to EP20) failed due to the breaking of the potting below the metal rod. In five other specimens (EP6, EP7, EP12, EP13 and EP16) the metal rod was not bonded to the insert. The other six specimens (EP5, EP8 to EP11 and EP15) failed due to the breaking of the potting/metal rod interface and in some cases combined to the fracture of the potting. Concerning the failure of the potting in the specimens, it's possible that it occurs due to traction or shear, but it's not easy to choose one.

On one hand, the fracture of the tested specimens occurs most of the time at ± 45°. Also, when the metal rod is being pulled-out, it clearly submits the potting to shear forces because of its geometry (white borders of EP1 in Fig. 21). On the other hand, there are some specimens on which the fracture of the potting happens at 0°. Moreover, during the tests, the failure of the potting was like a brittle material. However, these SPF are well known to present a brittle failure in traction and a plastic behavior under compression, which suggests that the shear failure should be a combination of both. Nevertheless, the brittle fracture failure is visibly dominant.

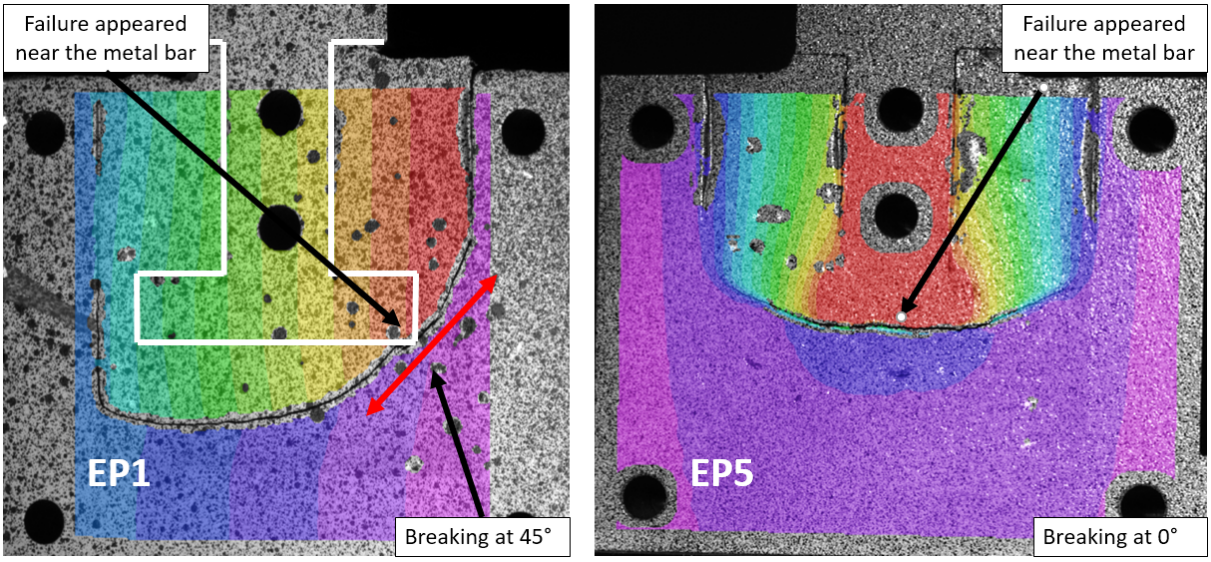

Fig. 21: Supposed potting failure due to traction of specimens EP1 and EP5.

However, another different type of failure scenario was observed for some tests (see Fig. 22). When the specimens were not degreased (EP6, EP7 and EP8) the pieces were not correctly bonded, as expected. Surprisingly, the same failure scenario appeared for specimens EP13, EP12 and EP16 which were correctly degreased before the manufacture. It is important to highlight that, while the final image of the failure where very similar (a detached rod), the failure mechanism that conducted to this failure are different. By observing the displacement fields of the tested specimens (using the VIC 3D system) important remarks can be made (see Fig. 22). It was clear that some of them were not bonded since the beginning (EP6, EP7 and EP8), surely due to the lack of degreasing (see specimen EP7 in Fig. 22). Some others were partially bonded (see specimen EP11 in Fig. 22), and it seems that when this happens the potting failure remains isolated and doesn't propagate, which results in gradually local failure instead of the suddenly fracture of the material. Finally, for the specimens with the excess of hardener (EP9 and EP11), it was observed that the pieces were well bonded but the potting became very soft and the rod detached gradually as like a cohesive failure.

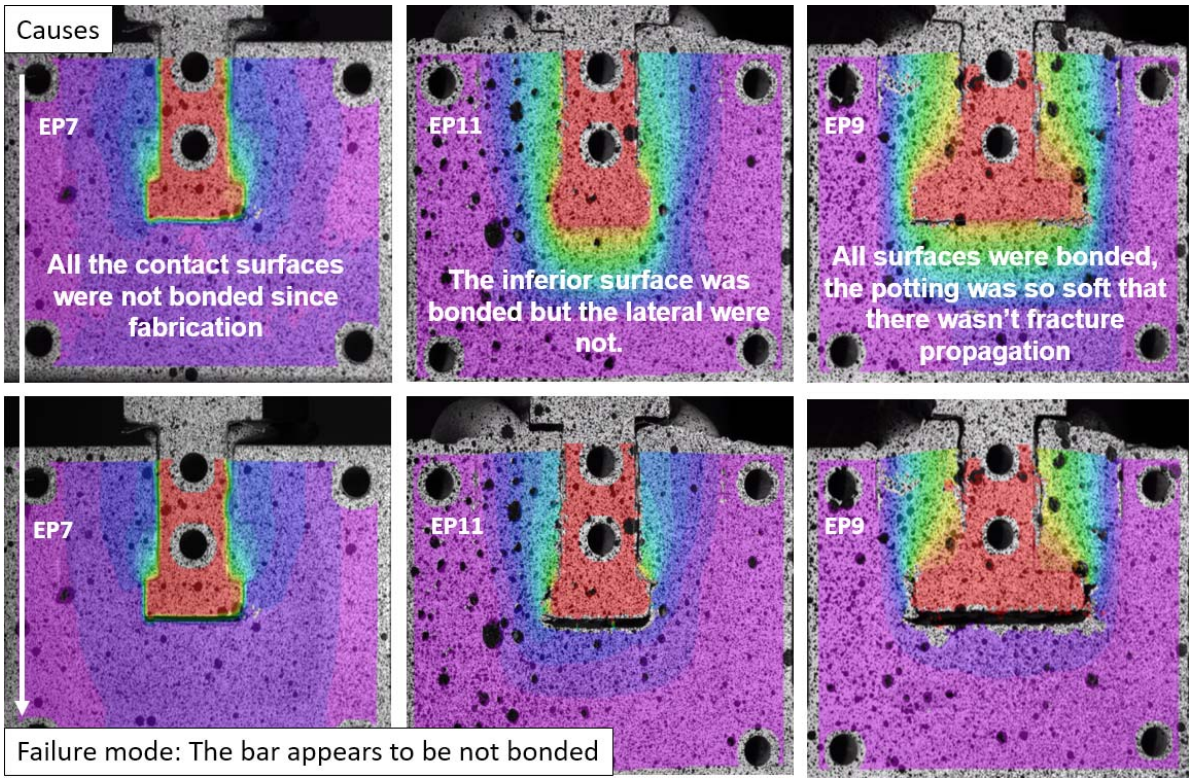

Fig. 22: Causes of the detaching of the metallic rod.

Nevertheless, even if the different failure evolutions were identified and described, the physical explanation of the defective bonding remains to be explained. Probably, it was because the polymerization reaction is exothermic and since the dilatation of both materials are different, small gaps might appear at the interface, and therefore the bonding between the parts was very weak or non-existent. Although these hypotheses might be too simple for such a complex phenomenon. Moreover, it is never worthless to mention that these adhesives are commonly designed to be applied as thin layers, not to be used as matrix for SPF and used to create a massive block to imbibe inserts.

Also, it's interesting to see that when 15% of micro-spheres were used (90.5 % of volume fraction) the potting was weakly bonded, or not bonded at all, to the metal rod (white color for the % of micro-spheres column of Table 5). This may suggest that for high micro-spheres concentrations, near to or beyond 15% of the ponderal weight, the potting loses its adhesive properties, although more tests are necessary to confirm this.

Finally, the last failure mode which is the breaking of the metal rod/potting interface appeared only on the specimens of type 4 (EP5, EP8, EP11 and EP15 denoted by letter B in Table 5, on which the size was similar to the metallic insert of the insert tests. This may suggest that because of the rod size, the stress at the interface increases, causing the interface failure.

4. Conclusions

As a part of a project to analyze the failure of inserts, this research is focused into clarifying the main aspects of the potting failure taking into consideration the influence of defects in the insert's pull-out strength. It is important to highlight the fact that the potting failure is strongly dependent of the defects that are introduced during its installation, and therefore both subjects are addressed in this research.

The first part of this work consisted into a review about defects in the potting of inserts, this is based in the experimental results of several authors. The evidence shows several defects that can be classified into the variations of the potting shape, the incomplete filling or air bubbles in the potting, the irregular borders of the potting and finally the defective bonding of the metallic insert. The analytical approaches for the insert design suggest that the potting zone is directly proportional to insert pull-out strength. However, this potting zone area varies according to the position of the honeycomb cells, and thus, the pull-out strength accordingly. In contrast, the incomplete filling of the cells seems to have no influence according to the tests results of Bunyawanichakul in [22]. Regarding the irregular borders of the potting, they might reduce the stability of the honeycomb cells and thus reduce their strength, although a proper study is still required and this subject is not addressed in this research. As for the defective bonding of the metallic inserts, it mostly appeared on inserts potted with SPF, but there were also cases when the insert was firmly bonded. Therefore, this defect is related to different type of potting failure modes. However, the actual causes of the

defective bonding problem and its consequences remained to be investigated. Then, the research was focused into study the causes of this defective bonding and two test campaigns were performed.

The first test campaign consisted in tensile and compressive test of the SPF to study their behavior under the variation of the microsphere concentration. It was seen that material tensile failure was brittle, while in compression the material presented a plastic behavior. Also, the microsphere concentration affected significantly the tensile modulus of the foam, while in compression the effect was almost imperceptible. Concerning the second test campaign, it consisted into the manufacturing and testing of several technological tests. Several aspects were included/used in the manufacturing of the technological specimens to observe the general influence that each aspect had into the bonding of the insert and the potting. They were; the inclusion of some fabrication mistakes, different polymerization temperatures, different microspheres concentrations and finally, two different insert sizes. Different hygrothermal conditions were not included in this study because these aspects were already studied in [21]. The first remark is that the failures of the technological specimens were indeed very similar to those observed in the failure of the pull-out tests performed by Bunyawanichakul in [22]. This confirms that the technological tests were representative of the different potting insert failures. Secondly, the results showed that the different potting's failure scenarios found by might have different causes, and two failure mechanisms were identified. When the insert is well bonded, the potting failure arrives when the maximal strength is reached in the potting or the interface between the potting and the insert, therefore it breaks (see Fig. 23). The procedures that resulted into a correct bonding were: polymerization of the specimens at room temperature during two days, correctly degreasing of the pieces and using a microspheres concentration of 11% or less of the ponderal weight of the adhesive.

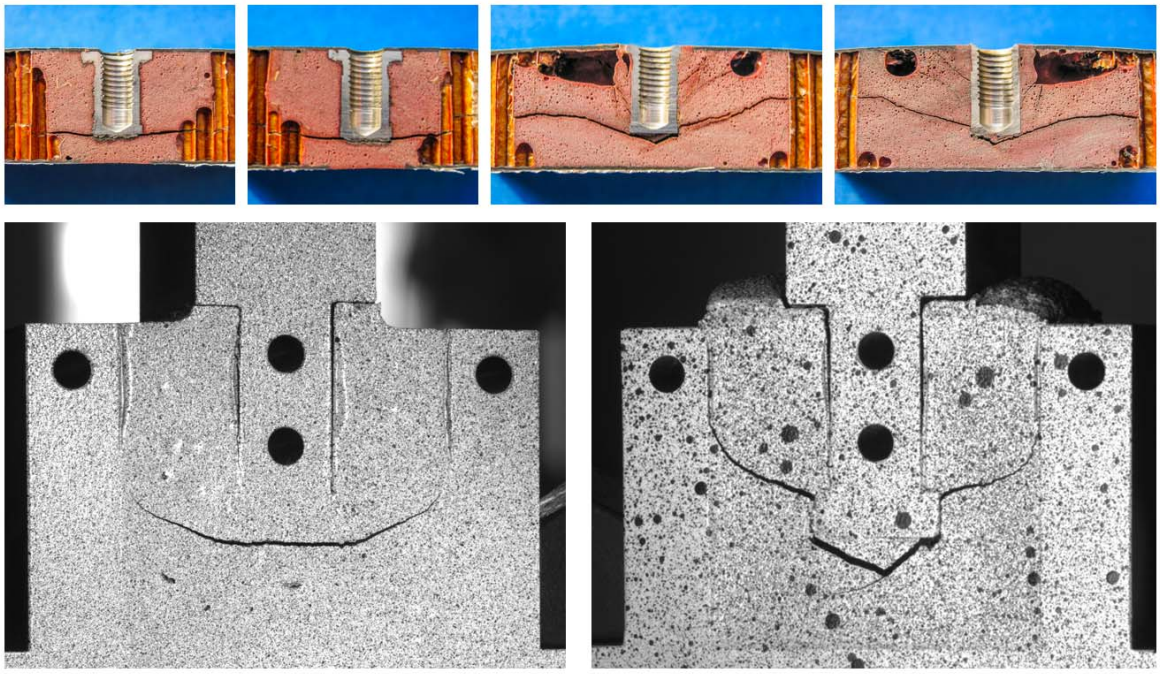

Fig. 23: Failure comparison: insert vs technological test with correct bonding.

The other failure mode appeared when the insert was not correctly bonded (see Fig. 24). This concentrates the pull-out load into the small contact zone between the potting and the insert. Therefore, even if the applied pull-out load is relatively low, since the contact area is small, the applied pressure becomes considerable high and the potting plasticizes very easily. The procedures that resulted into a defective bonding were identified: Lacking of degreasing of the parts, an excessive quantity of hardener in the adhesive and using a microspheres concentration near 15% of the ponderal weight of the adhesive (the potting is oversaturated of microspheres and loses his adhesive properties).

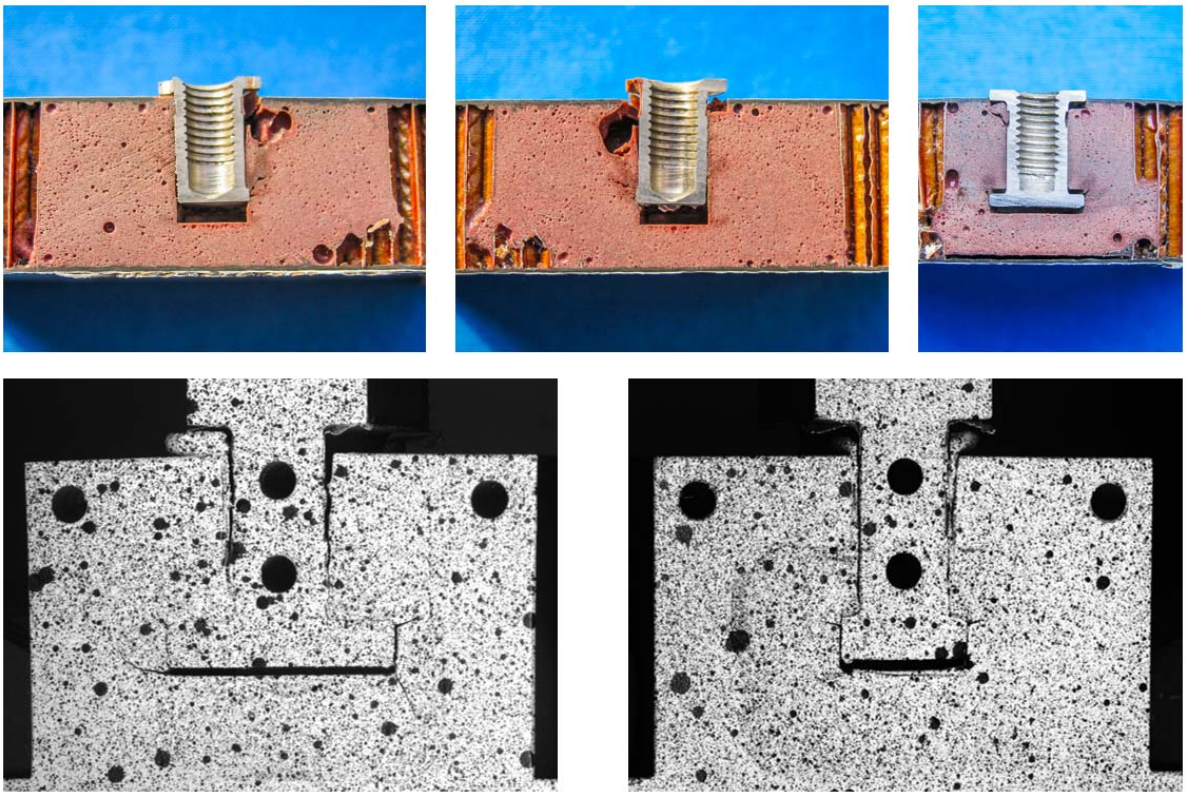

Fig. 24: Failure comparison: Insert vs technological test with defective bonding.

Moreover, the fact that the foam has a brittle failure under tension and an plastic in compression explains why the potting failure can be as a brittle material when is well bonded, because the potting is submitted to traction. In the other hand, when the insert is not well bonded, the potting is submitted to compression and the potting plasticizes. Nevertheless, it is important to highlight that also breaks due to shear. To show this, an insert specimens was observed under the microscope (see Fig. 25). The microspheres above the insert are clearly crushed due to compression and the potting is shear broken in the borders of the insert.

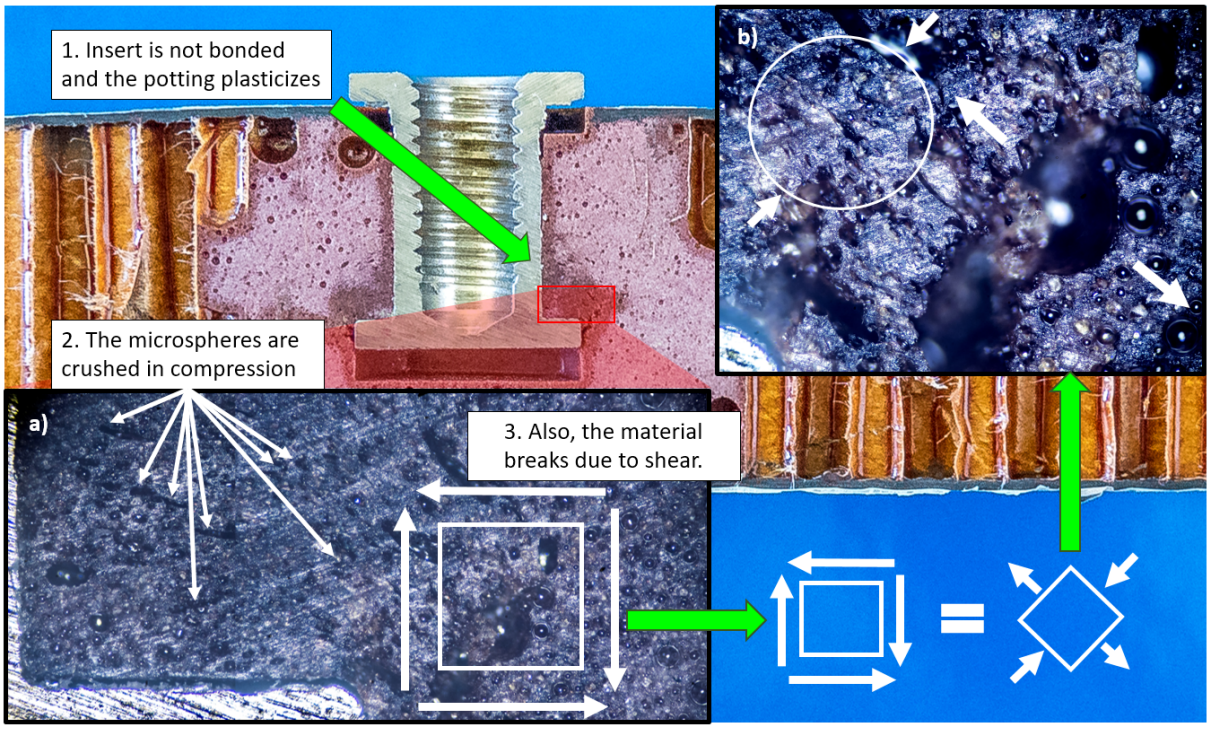

Fig. 25: Failure of the potting in shear.

Finally, most of researches highlight the fact that there is always an experimental scatter of around 20% in the pull-out strength of inserts installed using the same tools and materials. According them this variation can be attributed to the defects introduced when the insert is installed and potted into the sandwich panel. This research helps to clarify some of the cause of these variations and his consequences. The technological tests should also be useful to identify correct potting materials laws.

5. Acknowledgments

The present work was supported in part by the CONACYT from Mexico through the program “Becas Conacyt- Gobierno Frances”, the “Institut Clement Ader” and the INSA of Toulouse. This support is acknowledge with thanks.

References

[1] Kassapoglou C, *Design and Analysis of Composite Structures: With Applications to Aerospace Structures*. Wiley, 2011.

[2] Zenkert D, *The handbook of sandwich construction*. London: Emas, 1997.

[3] Gay D, *Composite Materials: Design and Applications, Third Edition*. CRC Press, 2014.

[4] Seemann R and Krause D, Numerical modelling of Nomex honeycomb sandwich cores at meso-scale level. *Compos Struct* 2017; 159: 702–718.

[5] Bunyawanichakul P, Castanié B, and Barrau JJ, Non-linear finite element analysis of inserts in composite sandwich structures. *Compos Part B Eng 2008;* 39(7–8): 1077–1092.

[6] Bunyawanichakul P, Castanié B, and Barrau JJ, Experimental and numerical analysis of inserts in sandwich structures. *Appl Compos Mater 2005; 12: 177–191.*.

[7] Mezeix L, Dols S, Bouvet C et al, Experimental analysis of impact and post-impact behaviour of inserts in Carbon sandwich structures. *J Sandw Struct Mater 2019;* 21(1): 135-153.

[8] European Space Agency, ESA PSS-03-1202 *Insert design handbooks*.

[9] MIL-HDBK-23A Structural Sandwich Composites Departement of defense USA, 1974.

[10] Rodriguez-Ramirez JDD, Castanié B and Bouvet C, Experimental and numerical analysis of the shear nonlinear behaviour of Nomex honeycomb core: Application to insert sizing. *Comp Struct 201*8;193:121–13.

[11] Smith B and Banerjee B. Reliability of inserts in sandwich composite panels. Compos Struct 2012; 94: 820–829..

[12] Raghu N, M. Battley M and Southward T, Strength Variability of Inserts in Sandwich Panels. *J Sand Struct Mater 2009; 11: 501–517.*

[13] Slimane S, Kebdani S, Boudjemai A, and Slimane A, Effect of position of tension-loaded inserts on honeycomb panels used for space applications. *Int J Interact Des Manuf 2018;12(2):* 393–408.

[14] European Space Agency, ECSS E HB 32 22A Insert Design Handbook, 2011.

[15] Wolff J, Trimpe F et al, Evaluation of an Analytical Approach Predicting the Transversal Failure Load of Insert Connections in Sandwich Structures. *in 20th International Conference on Composite Materials, Copenhagen, 19-24th July 2015.*

[16] Wolff J, Brysch M, and Hühne C, "Validity check of an analytical dimensioning approach for potted insert load introductions in honeycomb sandwich panels. *Comp Struct 2*018; 202:1195–1215.

[17] Seemann R and Krause D, Numerical modelling of partially potted inserts in honeycomb sandwich panels under pull-out loading. *Comp Struct 2018; 203:101–109, 2018.*

[18] Seemann R and Krause D, Virtual Testing of Nomex Honeycomb Sandwich Panel Inserts. *in 20th International Conference on Composite Materials, Copenhagen, 19-24th July 2015*.

[19] Rodríguez-Ramírez JDD, Castanié B, and Bouvet C, Damage Mechanics Modelling of the shear nonlinear behavior of Nomex honeycomb core. Application to sandwich beams. *Mech Adv Mater Struct, https://doi.org/10.1080/15376494.2018.1472351, On line*

[20] Heimbs S and Pein M, Failure behaviour of honeycomb sandwich corner joints and inserts. *Comp Struct 2009;89(4):575–588.*

[21] Bin Park Y, Kweon JH, and Choi JH, Failure characteristics of carbon/BMI-Nomex sandwich joints in various hygrothermal conditions. *Comp Part B Eng 2014;*60:213–

221.

[22] BUNYAWANICHAKUL P, Contribution à l'étude du comportement des inserts dans les structures sandwichs composites, PhD École Nationale Supérieure de l'Aéronautique et de l'Espace, 2005.

[23] Bunn P and Mottram JT, Manufacture and compression properties of syntactic foams. Composites 1993; 24(7):565–571.

[24] Heslehurst R, *Defects and Damage in Composite Materials and Structures*. CRC Press, 2014.

[25] Kumsantia P, Castanié P, and Bunyawanichakul P, An investigation of failure scenario of the metallic insert in sandwich structures. in *The First TSME International Conference on Mechanical Engineering*, 2010.

[26] Song KI, Choi JY et al, An experimental study of the insert joint strength of composite sandwich structures. *Comp Struct 2008;*86(1–3):107–113.

[27] Bianchi G, Aglietti GS, Richardson G, Static performance of hot bonded and cold bonded inserts in honeycomb panels. *J Sand Struct Mater 2011;*13(1):59–82.

[28] Kim BJ and Lee DG, Characteristics of joining inserts for composite sandwich panels," *Comp Struct 2008:* 86(1–3): 55–60.

[29] Lee SM, *Handbook of Composite Reinforcements*. Wiley, Palo Alto, California 1993.

[30] Gupta N, Ye R, and Porfiri M, Comparison of tensile and compressive characteristics of vinyl ester/glass microballoon syntactic foams. *Comp Part B* 2009;41:236–245.

[31] Bardella L, Malanca F et al, A micromechanical model for quasi-brittle compressive failure of glass-microballoons/thermoset-matrix syntactic foams. *J Eur Ceram Soc 2014;*34(11):2605–2616.

[32] Huang R and Li P, Elastic behaviour and failure mechanism in epoxy syntactic foams: The effect of glass microballoon volume fractions. *Comp Part B 2015:* 78: 401–408.

[33] Nian G, Shan Y et al, Failure analysis of syntactic foams: A computational model with cohesive law and XFEM. *Comp Part B* 2016:89:18-26.

[34] Rizzi E, Papa E and A. Corigliano, Mechanical behavior of a syntactic foam: Experiments and modeling. *Int J Solids Struct 2000;* 37(40): 5773–5794.